Sulfur-containing terpyridine derivatives: synthesis, coordination properties, and adsorption on the gold surface

R. B. Romashkina, A. G. Majouga, E. K. Beloglazkina, D. A. Pichugina, M. S. Askerka, A. A. Moiseeva, R. D. Rakhimov, and N. V. Zyk*

Department of Chemistry, M. V. Lomonosov Moscow State University, Build. 3, 1 Leninskie Gory, 119991 Moscow, Russian Federation. Fax: +7 (495) 932 8846. E-mail: bel@org.chem.msu.ru

Approaches to the synthesis of organic aurophilic ligands, *viz.*, sulfur-containing 2,2′:6′,2″-terpyridine derivatives, were developed. Complexation reactions of the terpyridine ligands having thiophenol, diaryl disulfide, and alkyl aryl sulfide fragments with Co^{II}, Ni^{II}, and Rh^{III} salts were studied. The structures of the coordination compounds obtained were established based on the elemental analysis data, density functional calculations, and electron spectroscopy. The structure of the complex of 4′-(4-methylsulfanyl)-2,2′:6′,2″-terpyridine with $Ni(BF_4)_2$ was also established by X-ray diffraction analysis. A method was proposed for the preparation of gold nanoparticle dimeric aggregates *via* coordination interactions of the ligands adsorbed on the gold nanoparticle surface with transition metal ions. A degree of nanoparticle aggregation upon their reaction with solutions of complex compounds of aurophilic nitrogen-containing ligands was determined by the concentration of the solution of the complex used.

Key words: sulfur-containing terpyridines, synthesis, adsorption on the gold surface, transition metal complexes, density functional calculations, electrochemistry, X-ray diffraction, terpyridine-containing disulfides.

In the last years, materials based on gold nanoparticles (NP) have become objects of serious study, since they are used in optical, nanoelectronic, and photonic devices, chemical and biological sensors, and catalysts.[1—3] The major problem is that metal NP are unstable in solution and have tendency to agglomeration. To prepare stable NP, it is necessary to use stabilizing agents, which, being adsorbed on the nanoparticle surface, would prevent their association. Sulfur-containing organic compounds (thiols, sulfides, disulfides, *etc.*) are most often used as gold NP stabilizers, which undergo chemosorption on the gold surface with the formation of an Au—S covalent bond.[4]

The modification of gold NP with functionalized organic ligands allows one to impart new useful properties to the nanoparticles. If terminal donor groups are present in the ligands, metal complexes can form on the NP surface.

We proposed a new method for the preparation of dimeric and trimeric NP aggregates *via* coordination interactions of ligands adsorbed on their surface with transition metal ions.[5] Examples of the preparation of such aggregates described in the literature are based on the reaction of complementary parts of DNA molecules,[6] electrostatic interactions,[7] hydrogen bonding,[8] or covalent interactions of polythiols with several NP.[9] However, in most cases such interactions proceed with low yields and lead to the irreversible binding of NP to each other. The advantage of our method is the controlled preparation of NP ensembles with different degrees of aggregation and reversibility of their formation, since when a stronger complexing agent is added to the system, it can bind to the metal ion and the starting monomeric NP can be regenerated.

The purpose of the present work was to synthesize new aurophilic terpyridine ligands and study their reactions with transition metal ions; investigate adsorption of the ligands and coordination compounds obtained on the surface of gold electrodes and gold NP by a combination of physicochemical and quantum mechanical methods, as well as to find a possibility of using this type ligands for the preparation of gold NP dimeric aggregates.

2,2′:6′,2″-Terpyridine derivatives (TerPy) containing three donor nitrogen atoms are widely used as ligands in coordination chemistry. Such ligands are able to coordinate metal ions of different nature and form complexes of the composition 2 : 1 or 1 : 1 depending on the metal type and reaction conditions.[10,11] Bis-terpyridine complexes with symmetric structure are commonly formed when Co^{II}, Ni^{II}, Cu^{II}, Zn^{II}, Fe^{II}, *etc.* are involved in complexation reactions. In most of such coordination compounds of the composition $[M(TerPy)_2X_2]$ ($X = Cl^-$, ClO_4^-, PF_6^-, *etc.*), the metal ion is in the pseudooctahedral environment, with six nitrogen atoms of two terpyridine fragments being involved in the complexation.[5,10] However,

Published in Russian in *Izvestiya Akademii Nauk. Seriya Khimicheskaya,* No. 12, pp. 2244—2260, December, 2012.

1066-5285/12/6112-2265

usually it is impossible to use these metals for the binding of two different terpyridine fragments upon a sequential introduction of the ligands, and the complexes of the composition 2 : 1 are formed independently of the initial ligand : metal salt molar ratio. The involvement of these metal salts in the complexation reaction with a mixture of two different ligands gives mixtures of homo- and heteroligand complexes.

A strategy for the preparation of bis-terpyridine complexes with the unsymmetric structure was developed based on the step-by-step introduction of two ligand molecules into the complexation reaction with metal ions (Rh^{III}, Ru^{III}, Os^{III}, more seldom Co^{II}),[11–14] which in the first step are able to form complexes [M(TerPy)X_3] (X = Hal). The use in the second step of reducing agents, for example *N*-ethylmorpholine, allows one to obtain the corresponding unsymmetric complexes, in which the metal ion has oxidation state +2.

In the present work, we describe new bifunctional aurophilic TerPy derivatives, which are able of both being adsorbed on the gold surface and reacting with transition metal ions to form A-type complex compounds.

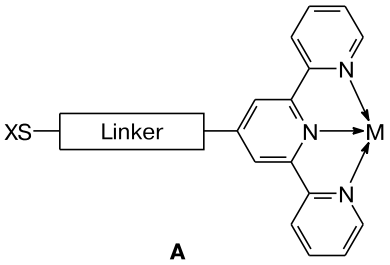

A

XS = SR, SH, S—SR; R = Me, Bu^t

The ligands obtained contained aryl and vinylaryl substituents as the linkers.

Results and Discussion

Synthesis of ligands and complexes. 2,2′:6′,2″-Terpyridine derivatives **1** and **2** containing an aromatic linker were obtained by the Kröhnke condensation from 2-acetylpyridine and aromatic aldehydes containing methylthio or *tert*-butylthio groups (Scheme 1).

To obtain thiol **3**, terpyridine **2** was hydrolyzed with hydrochloric acid. A mixture of thiol **3** and disulfide **4** was isolated as the hydrolysis product. To obtain the individual thiol, disulfide **4** was reduced with triphenylphosphine without isolation from the reaction mixture (Scheme 2).

The terpyridine ligands containing a vinylaryl fragment were obtained according to Scheme 3. The reaction of 4′-(4-methylphenyl)-2,2′:6′,2″-terpyridine (**5**) with *N*-bromosuccinimide led to a mixture of the target monobromide **6** and dibromide **7** (see Scheme 3). Monobromide **6** was isolated from the mixture and involved in the Arbuzov reaction with triethyl phosphite to obtain phosphonate **8**. The Horner—Wadsworth—Emmons reaction of compound **8** with methylthio- and *tert*-butylthio-substituted aromatic aldehydes gave the target terpyridines **9** and **10** (Scheme 4), which contained vinylaryl linkers in their structures. The spin-spin coupling constants of the vinyl protons in the ^{1}H NMR spectra of compounds **9** and **10** are equal to ~16 Hz, that confirms the *E*-configuration of the double bond in the compounds obtained.

The complex of ligand **1** with cobalt(II) hexafluorophosphate (**11**) was synthesized according to Scheme 5. Ligand **1** was refluxed with $Co(NO_3)_2 \cdot 6H_2O$ in methanol followed by the addition of a saturated solution of ammonium hexafluorophosphate.

Structurally related Co^{II} and Ni^{II} complexes were obtained from ligands **1**, **2**, **9**, **10** and $Co(ClO_4)_2 \cdot 6H_2O$ or $Ni(BF_4)_2 \cdot 6H_2O$ by reflux in methanol (Scheme 6).

The structure of complex **14** was confirmed by X-ray diffraction (the crystallographic data, X-ray diffraction data collection and structure refinement statistics are given in Table 1), as well as by quantum chemical simulation. According to the crystallographic data (Fig. 1, Table 2), the metal atom in the structure of complex **14** coordinates six N atoms of two terpyridine fragments and has a distorted octahedral ligand environment, similarly to other known M^{II} terpyridine complexes.[5,10] Optimization of the

Scheme 1

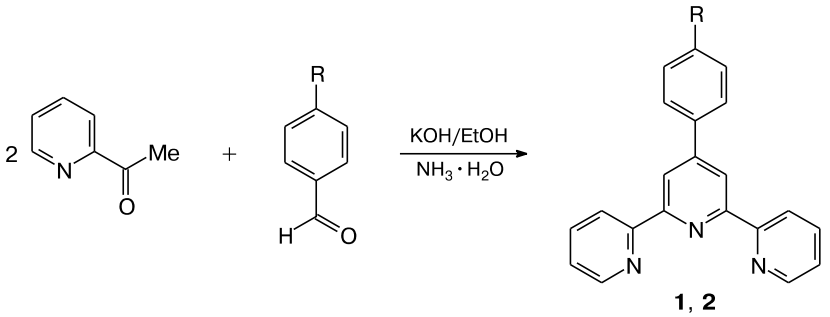

1, **2**

R = SMe (**1**), SBu^t (**2**)
Yield (%): 42 (**1**), 45 (**2**).

Scheme 2

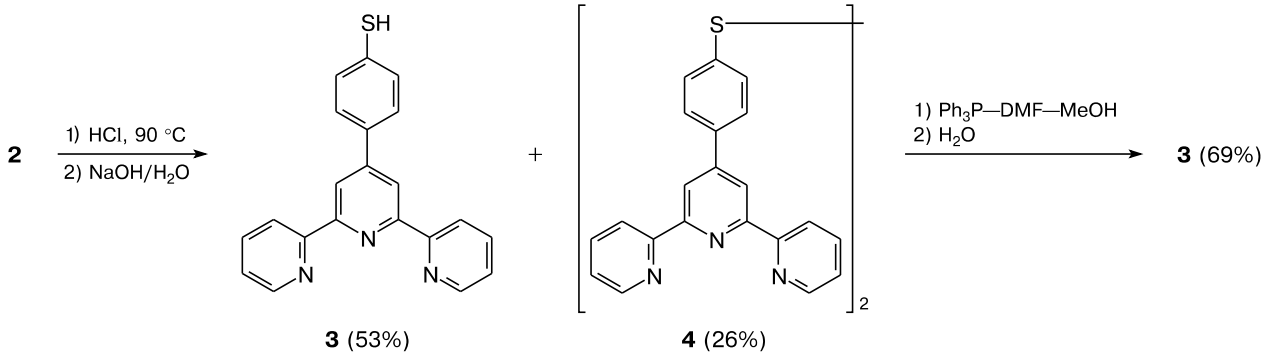

Scheme 3

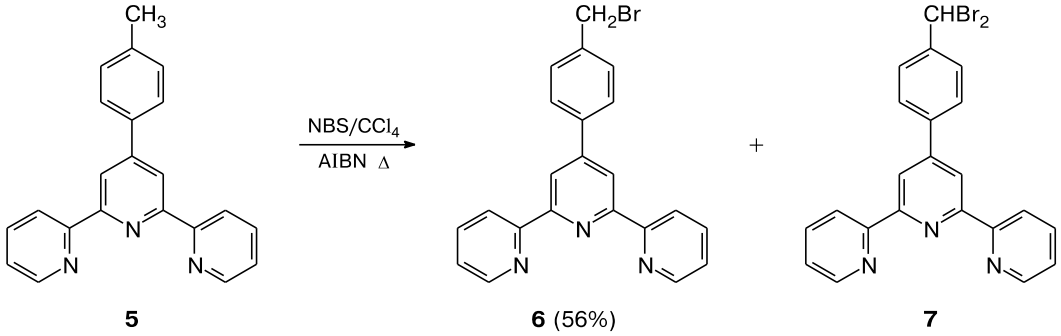

Scheme 4

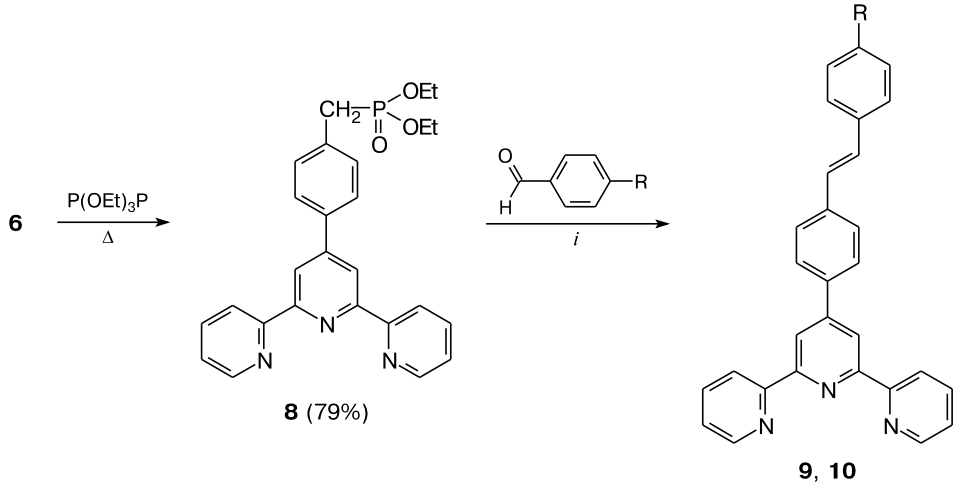

i. Bu^{t}OK, toluene, Δ.

R = SMe (**9**), SBu^t (**10**). Yield (%): 64 (**9**), 57 (**10**)

structure of complex **14** by the density functional theory revealed that the conformations of the nonrigid fragments and the environment of the central atom are similar to those found for the solid phase. The calculated geometric parameters agree with the results of the X-ray diffraction analysis with good accuracy. Thus, an average Ni—N distance obtained by X-ray analysis (2.074 Å) is close to the calculated distance (2.098 Å).

Scheme 5

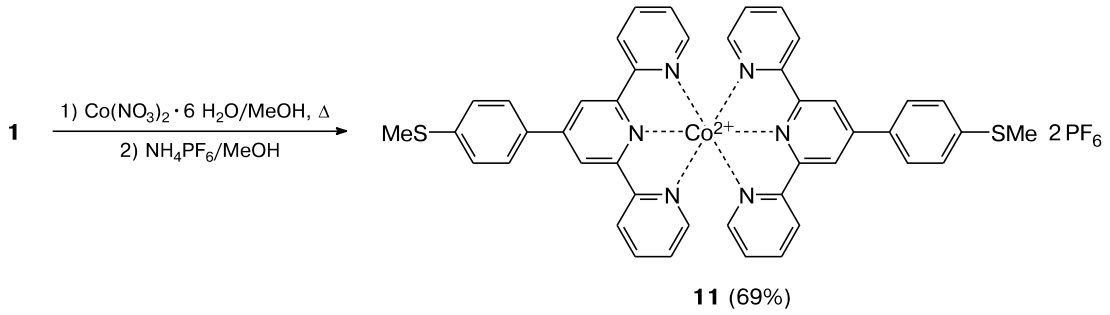

11 (69%)

Scheme 6

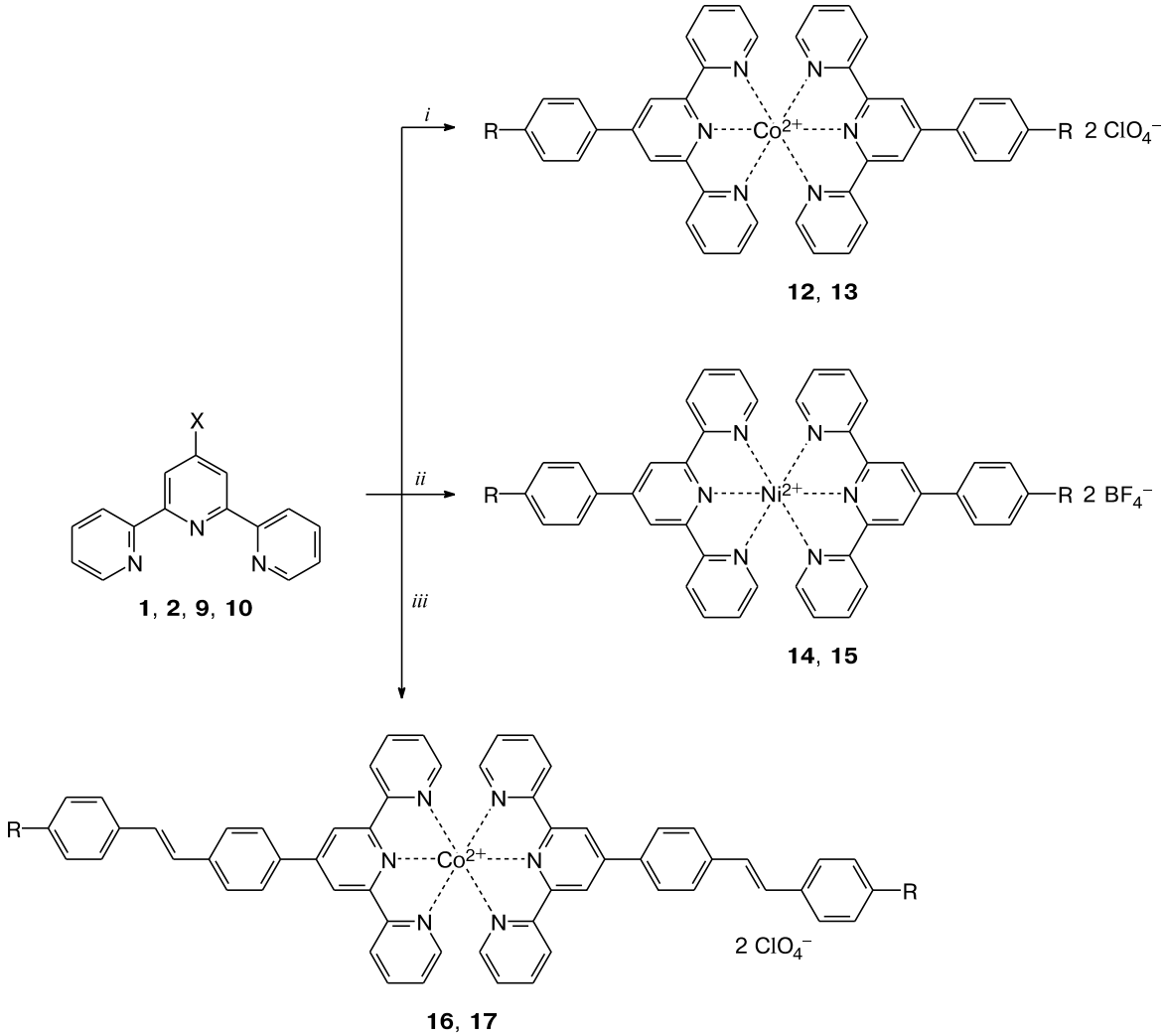

12, **13**

14, **15**

16, **17**

i. $Co(ClO_4)_2 \cdot 6H_2O$, MeOH, Δ; *ii*. $Ni(BF_4)_2 \cdot 6H_2O$, MeOH, Δ; *iii*. $Co(ClO_4)_2 \cdot 6H_2O$, MeOH, Δ.

R = SMe (**12**, **14**, **16**), SBu^t (**13**, **15**, **17**)

Yield (%): 89 (**12**), 83 (**13**), 61 (**14**), 57 (**15**), 48 (**16**), 66 (**17**).

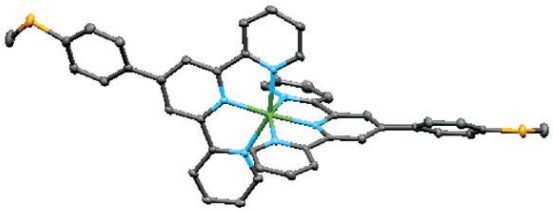

Fig. 1. Molecular structure of the $[Ni(\mathbf{1})_2]^{2+}$ cation (in complex **14**) according to the X-ray diffraction data.
Note. Fig. 1 is available in full color in the on-line version of the journal (http://www.springerlink.com/issn/1573-9171/current).

The terpyridine ligands containing thiol and disulfide groups were involved in the complexation reactions with cobalt(II) perchlorate. According to the elemental analysis data, a complex of the composition L : M = 1 : 1 was obtained in the case of disulfide ligand **4**, whereas in the case of thiol **3** it was a complex with the ratio L : M = 2 : 1 (Scheme 7). The optimization of the structure of the complexes with such a ratio by the density functional theory showed that complexes **18** and **19**, like complex **14**, have the octahedral ligand environment. Figure 2 shows a suggested structure for complex **19**. The calculated average Co—N distance was 2.041 Å.

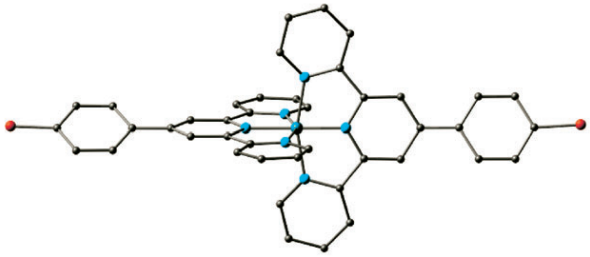

Fig. 2. A structural fragment of the Co^{2+} complex with two molecules of thiol **3** (compound **19**) optimized by the density functional theory. Hydrogen atoms are not shown.
Note. Fig. 2 is available in full color in the on-line version of the journal (http://www.springerlink.com/issn/1573-9171/current).

In this case, we failed to obtain crystals suitable for X-ray diffraction studies, since the complexes have an extremely low solubility in organic solvents. In the case of disulfide complex **18**, this fact is possibly explained by its polymeric structure (see Scheme 7).

The mixed-ligand complexes of terpyridine derivatives **1** and **2** with Rh^{III} ions binding two different terpyridine ligands were synthesized according to Scheme 8. When refluxed with $RhCl_3$ in aqueous ethanol, ligands **1** and **2** formed the $[Rh(TerPy)Cl_3]$ complexes, which were further involved in the reaction with 1,4-bis(terpyridin-4′-yl)benzene (**20**).

Adsorption of the ligands and coordination compounds obtained on the gold surface. The electrochemical studies of the terpyridine ligands and their complexes were carried out by cyclic voltammetry (CV) using glassy carbon (GC) and gold electrodes.

The reduction of alkyl aryl sulfide ligands **1**, **2**, **9**, and **10** on the GC electrode takes place in three steps at the potentials E_{pc} from −1.79 to −1.92 V corresponding to the reduction potentials of the terpyridine fragment[15] (Table 3, Fig. 3, *a*). The oxidation of compounds **1** and **2** occurs in

Table 1. Crystallographic data, X-ray diffraction data collection and structure refinement ststistics for of compound **14**

Parameter	Value
Molecular formula	$C_{44}H_{34}B_2F_8N_6NiS_2$
Molecular weight	943.22
T/K	100(2)
Crystal size/mm	0.42×0.31×0.24
Crystal shape	Red prisms
Crystal system	Monoclinic
Space group	$P2_1/c$
Unit cell parameters	
a/Å	33.8990(16)
b/Å	15.1523(7)
c/Å	15.9273(8)
α/deg	95.4100(10)
V/Å^3	8144.6(7)
Z	8
d_{calc}/g cm^{-3}	1.538
Absorption coefficient, μ/mm^{-1}	0.659
F(000)	3856
Scanning range, θ_{min}—θ_{max}/deg	0.60—29.00
h, k, l ranges	$-46 \le h \le 43$ $-20 \le k \le 20$ $-21 \le l \le 21$
Number of measured reflections	21631
Number of unique reflections	13825
R_{int}	0.0393
Number of refinement variables	1139
Goodness of fit on F^2	0.977
R_1 ($I > 2\sigma(I)$)	0.0525
wR_2 ($I > 2\sigma(I)$)	0.1681
R_1 (all data)	0.1015
wR_2 (all data)	0.1364

Table 2. Selected interatomic distances (d) and bond angles (ω) for compound **14**

Bond distance	d/Å	Bond angle	ω/deg
Ni(1)—N(1A)	1.998(2)	N(1A)—Ni(1)—N(1)	173.48(9)
Ni(1)—N(1)	2.000(2)	N(1A)—Ni(1)—N(2A)	77.26(9)
Ni(1)—N(2A)	2.108(2)	N(1)—Ni(1)—N(2A)	109.23(9)
Ni(1)—N(2)	2.109(2)	N(1A)—Ni(1)—N(2)	103.08(9)
Ni(1)—N(3)	2.110(2)	N(1)—Ni(1)—N(2)	77.84(9)
Ni(1)—N(3A)	2.118(2)	N(2A)—Ni(1)—N(2)	91.60(9)
S(1)—C(19)	1.759(3)	N(1A)—Ni(1)—N(3)	101.92(9)
S(1)—C(22)	1.793(3)	N(2A)—Ni(1)—N(3)	91.67(9)

Scheme 7

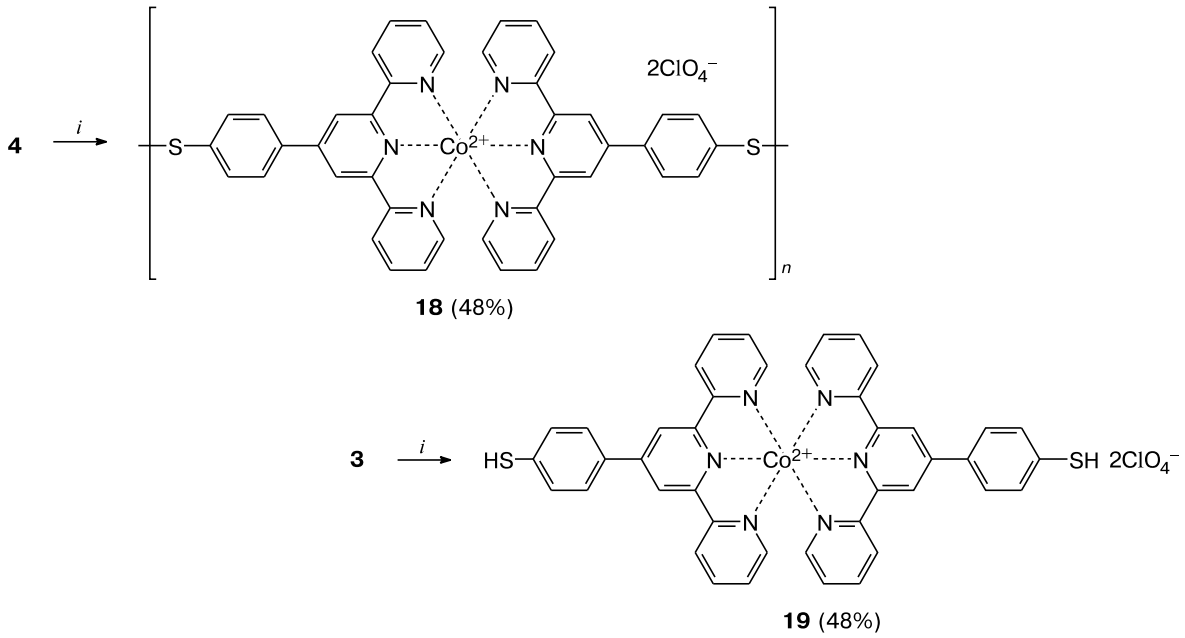

i. $Co(ClO_4)_2 \cdot 6H_2O$, MeOH, Δ.

Scheme 8

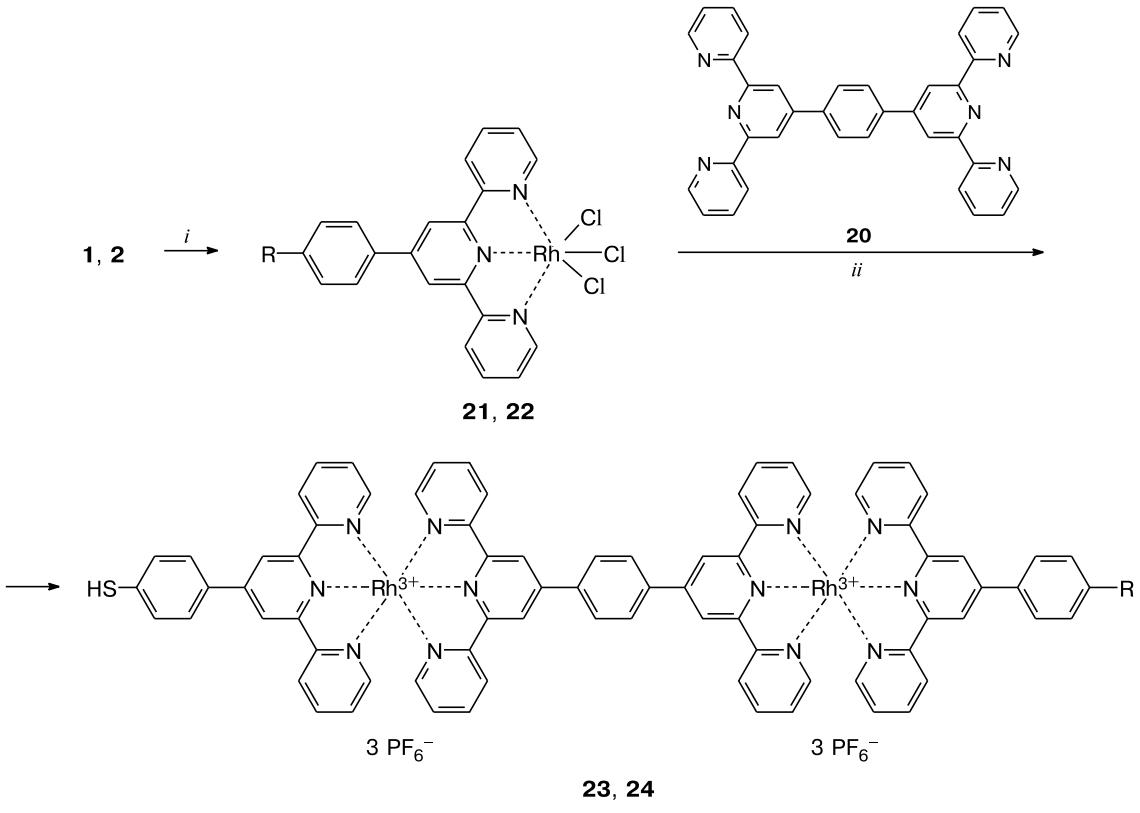

i. $RhCl_3$, $EtOH/H_2O$, Δ; *ii*. 1) $EtOH/H_2O$, 2) NH_4PF_6, Δ.

R = SMe (**21**, **23**), SBu^t (**22**, **24**)
Yield (%): 36 (**21**), 30 (**22**), 45 (**23**), 44 (**24**).

Table 3. Electrochemical reduction (E^{Red}) and oxidation (E^{Ox}) potentials of terpyridine ligands and complexes on GC and Au electrodes measured by CV relative to Ag|AgCl|KCl(sat.)[a]

Compoum	Electrode	E_p^{Ox}	$-E_p^{Red}$
		V	
1	GC	1.27	1.92
			2.12
			2.30 (2.13)
1	Au	1.50	1.39 (ads.)
(ads.)			1.74 (1.65)
2	GC	1.13[b]	1.79
			2.07
			2.71 (2.21)
2	Au		0.93 (Au—S)
(ads.)			1.50 (ads. N)
			1.76
			2.01
4	GC	0.67	0.95 (S—S)
		1.11	1.74
			1.99 (1.87)
			2.26 (2.18)
			2.37
4	Au		0.82 (Au—S)
(ads.)			1.22 (S—S)
			1.59
9	GC	0.33	0.65 (0.59)
		(0.24)	1.44 (1.37)

Compound	Electrode	E_p^{Ox}	$-E_p^{Red}$
		V	
9	GC		1.84 (1.72)
(ads.)			2.14
	Au	0.37	0.74 (0.61)
		(0.22)	1.48 (1.36)
			1.84 (1.68)
			2.03
10	GC	0.42	0.74 (0.55)
		(0.24)	1.44 (1.28)
			1.80
			2.04
10	Au	0.37 (0.18)	0.77 (0.58)
(ads.)		1.18	1.19
			1.41 (1.29)
			1.54
			1.80
			2.04
12	GC	1.36	1.68 (1.52)
		1.54	1.86 (1.63)
			1.96 (1.84)
12	Au	1.36	1.10 (ads.)
(ads.)			1.68 (1.52)
			2.04 (1.86)

Compound	Electrode	E_p^{Ox}	$-E_p^{Red}$
		V	
12[c]	Au	1.14	0.82 (0.54)
		1.54	1.63 (1.58)
			1.80
13	Pt	1.54	1.70 (1.53)
		(0.28; 0.26; 0.84)	1.96 (1.86)
13	Au	1.36 (0.62)	0.76 (Au—S)
(ads.)			1.64
			1.92
13[d]		0.96	0.84 (0.63)
		1.36 (0.61)	1.19
			1.70
18	GC	0.31 (0.28)	0.63
			0.82 (S—S)
			1.13
			1.61 (1.56)
			2.02 (1.86)
18	Au		0.57
(ads.)			0.78 (Au—S)
			1.16
			1.61
			1.84
			2.01

[a] DMF, 0.1 *M* Bu_4NClO_4, 200 mV s^{-1}. The reverse peak potentials are given in parentheses. E_p is the peak potential.
[b] Only in the second and subsequent potential scans; corresponded to the oxidation of the S—S fragment.
[c] Adsorbed ligand **1**, Au electrode + $Co(ClO_4)_2$.
[d] Adsorbed ligand **2**, Au electrode + $Co(ClO_4)_2$.

one irreversible step at E_{pa} = 1.27 and 1.13 V, respectively, apparently, at the sulfide fragment.[16,17] For compounds **9** and **10**, there is a second peak in the oxidation region corresponding probably to the oxidation of the C=C bond. Note that in the reverse potential scan, a reduction peak at E_{pc} = −0.94 V appears in the CV curve of ligand **2** after passing the anodic peak potential. A similar peak was found in the CV curve of disulfide **4**; it corresponded to the reduction of the S—S fragment. Such a peak was absent in the CV curve of methyl derivative **1**. It is obvious that the radical cation formed by the oxidation of sulfide **2** decomposes to radical $ArS^{\bullet}$, subsequently giving disulfide **4**, and the stable *tert*-butyl cation (Scheme 9). In the case of ligand **1** such a decomposition, which would have led to a considerably less stable methyl cation, does not take place.

Scheme 9

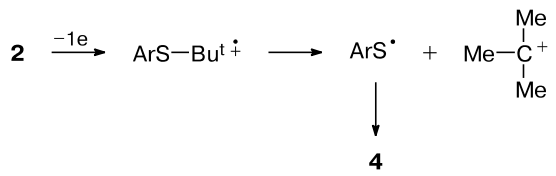

The first step of the reduction of disulfide **4** involves apparently the S—S bond (E_{pc} = −0.95 V). Further reduction steps take place at the terpyridine fragments.

In the CV curves of cobalt-containing complexes **12**, **13**, and **18**, in contrast to the CV curve of the free ligands, two additional peaks corresponding to the transitions $Co^{II} \rightarrow Co^{I}$ and $Co^{I} \rightarrow Co^{0}$ are present in the cathodic scan (see Table 3, Fig. 3). In the case of complexes **12** and **13**, both transitions are reversible. The reduced forms of the complexes containing Co^{I} and Co^{0} are stable in solution. This is confirmed by the absence of the oxidative desorption of metallic Co from the electrode surface in the CV curves during the reverse potential scans.

In the CV curves of sulfide complexes **12** and **13**, a reversible peak of the $Co^{III} \rightarrow Co^{II}$ transition is also observed in the oxidation region. The presence of three reversible redox transitions at low potentials makes complexes **12** and **13** promising for their studies as catalysts for redox reactions.

To confirm the adsorption of the compounds under study on the Au surface, the Au electrode was kept for 20 h in solution of a ligand or a complex ($C = 10^{-3}$ mol L^{-1}), then washed with acetone and dried. The thus treated elec-

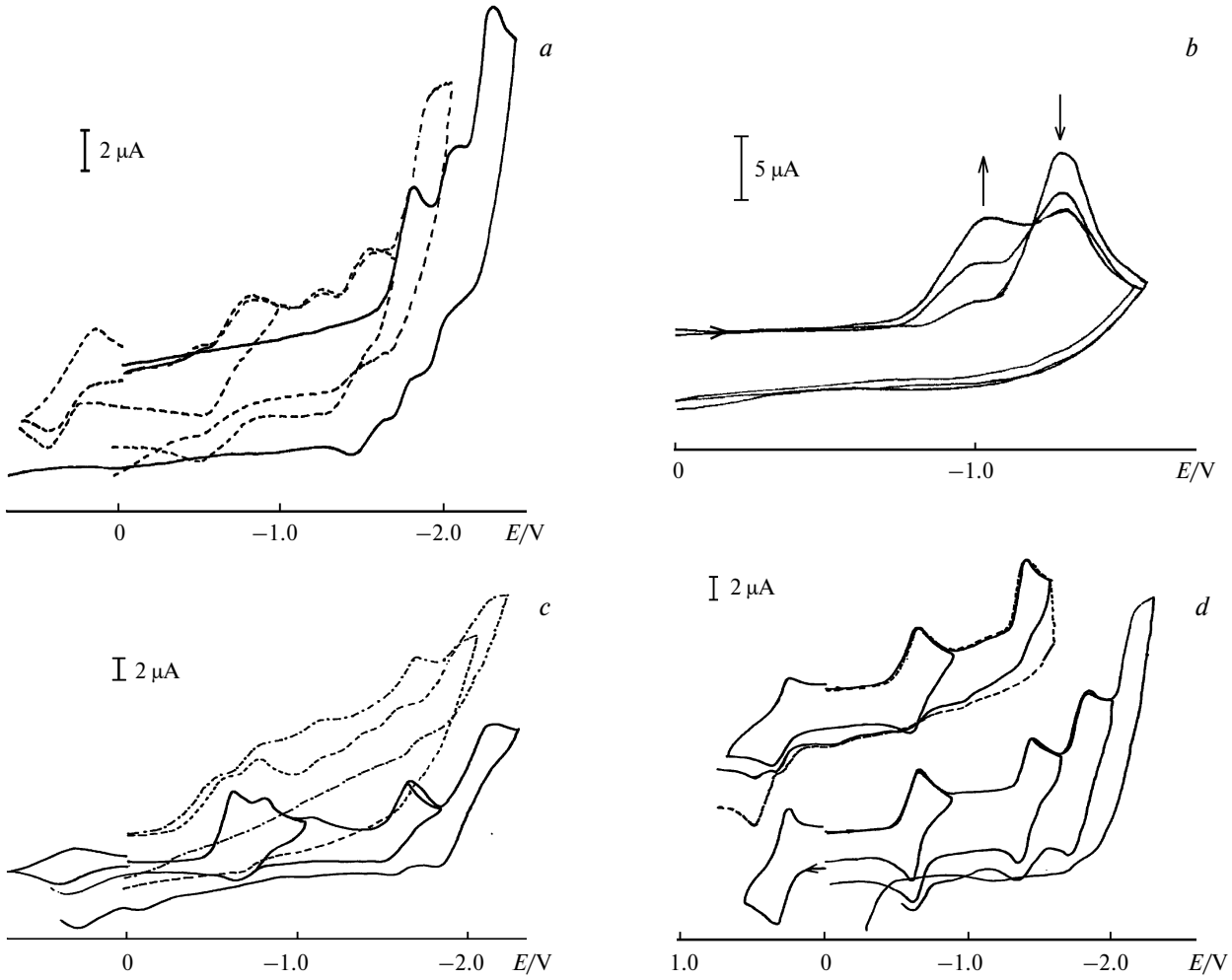

Fig. 3. Cyclic voltammograms (DMF, the concentration of solution $5 \cdot 10^{-4}$, 0.1 *M* Bu_4NClO_4): *a* ligand **2**, GC electrode (solid line), and complex **13**, Au electrode (dashed line); *b* ligand **4**, Au electrode (the arrows in the figure show the change in the peak intensities with time; the first curve was recorded in 1 min, the last in 20 min after dipping the electrode in the solution); *c* complex **18**, Au electrode, solution (solid line), the same complex adsorbed on the Au electrode (dashed line), and complex formed on the surface of the Au electrode upon keeping the electrode with ligand **2** adsorbed on it in the solution of $Co(ClO_4)_2$ (dotted-and-dashed line); *d* complex **12**, GC electrode (lower curves) and the same complex, GC electrode, in the presence of excess of Bu^nI (upper curves).

trode was placed in the pure supporting electrolyte to measure a CV curve.

The reduction peaks of sulfide ligands **1**, **2**, **9**, and **10** on the Au electrode were slightly shifted to the anodic side as compared to the GC electrode. For *tert*-butyl-containing ligands **2** and **10**, an additional reduction peak of the Au—S bond was observed in the CV curve at $E_{pc} = -0.93$ V. This is an evidence of a possibility of its adsorption on the gold surface with the cleavage of the C—S bond. However, the initial adsorption process of ligands **2** and **10** on Au proceeds apparently due to the coordination of the nitrogen atoms of the terpyridine fragment, similarly to that described in the work,[18] and only after that the "reorientation" occurs with adsorption of the sulfur atom and the resulting formation of the Au—S bond. This suggestion is supported by the fact that the CV curve measured during the first hours of the contact of the Au electrode with the solution of **2** has a reduction peak of the terpyridine fragment coordinated to Au at $E_{pc} = -1.47$ V, which gradually disappears, being completely replaced with the peak $E_{pc} = -0.82$ V approximately after 20 h (Scheme 10).

For SMe-substituted terpyridines **1** and **9** no reduction peak of the Au—S fragment is observed in the CV; thus, their chemosorption with the formation of the Au—S bond does not occur.

To validate this suggestion, we calculated the bond energy of SMe-substituted terpyridine **9** with the Au_{20} gold cluster. This cluster was chosen as a model due to its high stability;[19] the atoms on the cluster faces follow the Au surface motif. To determine the most probable sorption centers, a visualization of the molecular orbitals of the

Scheme 10

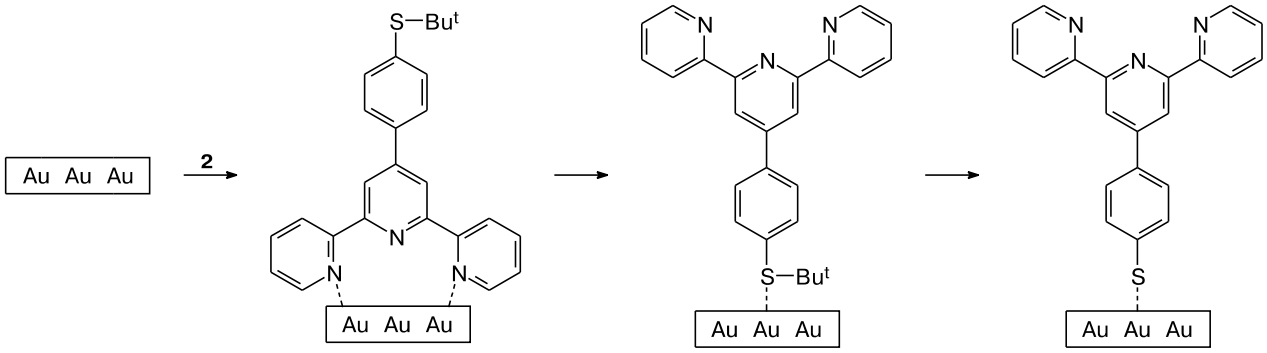

Au_{20} cluster was carried out. The calculations performed[19] showed that the bonding of the gold clusters with the ligands is effected by means of electron density transfer to the LUMO of the cluster. The shape of the LUMO of the Au_{20} cluster (Fig. 4) shows that the largest deficiency of electron density is experienced by the apical gold atom and, consequently, it is a suggested active center.

The optimized structures of the thiol complexes with the Au_{20} cluster are shown in Fig. 5. The bond energy of the thiol with the cluster upon its coordination by the terpyridine fragment (see Fig. 5, *a*) is higher than that involving the thiol fragment (see Fig. 5, *b*). This is apparently due to the formation of three Au—N donor-acceptor bonds. The calculated bond energies are equal to 146 and 135 kJ mol^{-1} for the complexes shown in Figs 5*a* and 5*b*, respectively. To sum up, the sorption of the SMe-substituted terpyridine on the gold surface with the participation of the terpyridine fragment, rather than the sulfur atom, is thermodynamically more favorable.

The adsorption of complex **13** on the gold electrode is also accompanied by the formation of the Au—S bond

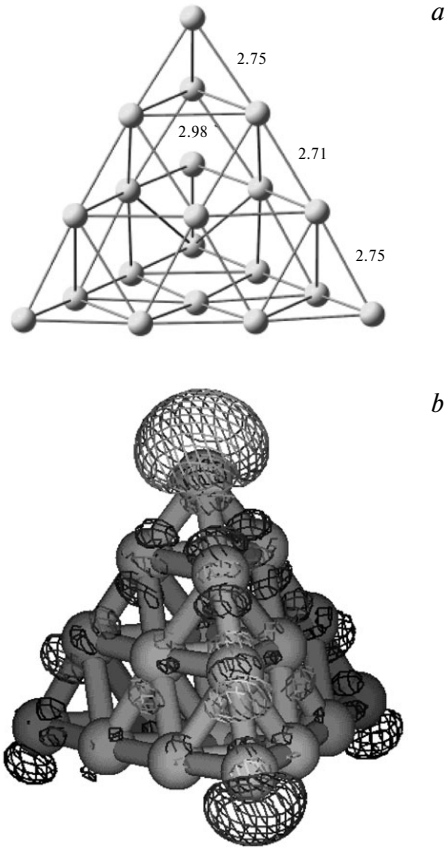

Fig. 4. Structure of the Au_{20} cluster (*a*) and visualization of its molecular orbitals (*b*).

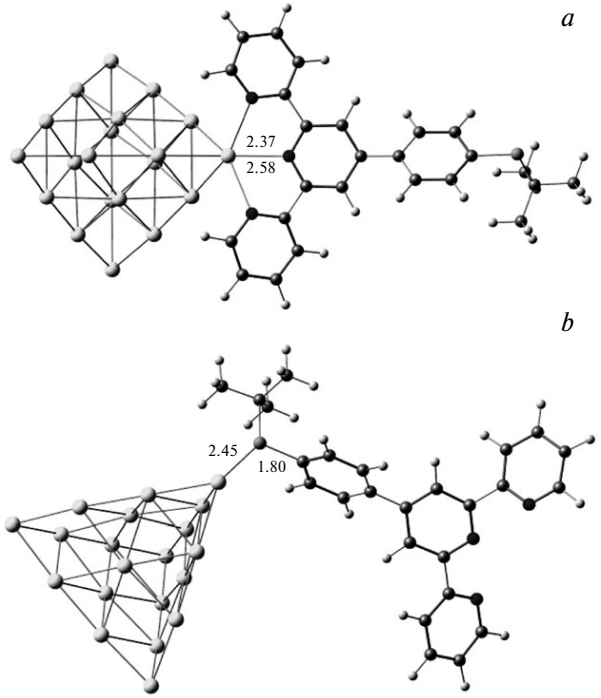

Fig. 5. Optimized structures of SMe-substituted terpyridine complexes **9** with the Au_{20} cluster: coordination by the terpyridine fragment (*a*) and the sulfur atom (*b*). The calculated distances are given in Angstroms.

(the reduction peak at E_{pc} = –0.82 V; see Table 3 and Fig. 3, *b*). According to the CV data, the structure of compound **13** in solution is identical to that on the surface of the gold electrode. Apparently, the structure of complex **13** adsorbed on the gold surface corresponds to that shown in Fig. 6.

However, according to the CV data, the keeping the Au electrode with ligand **2** chemosorbed on it in the solution of $Co(ClO_4)_2$ led to the complex with a different structure, which is similar to that obtained upon adsorption of complex **18** (Fig. 3, *c*). A probable structure of this coordination compound is presented in Scheme 11.

Scheme 11

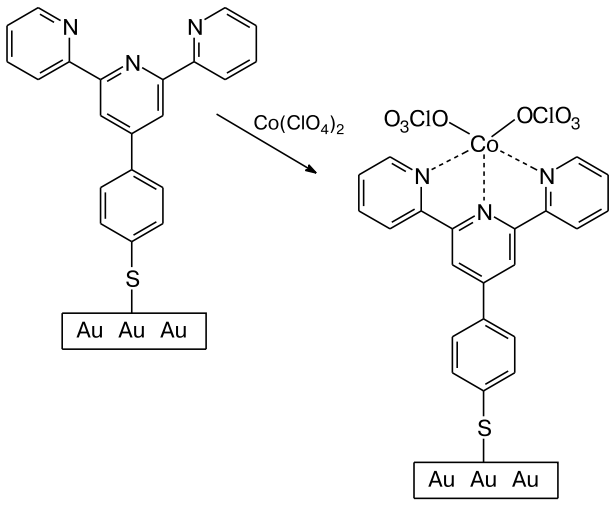

The studies of redox processes on the Au electrode for ligand **4** already in the first reverse scans of the CV curve also showed the presence of an additional (as compared to the GC electrode) cathodic peak at E_{pc} = –0.82 V corresponding to the reduction of the Au—S bond, which was formed as a result of chemosorption of compound **4** on the surface of the electrode. A peak corresponding to the reduction of the disulfide bond (E_{pc} = –1.22 V) was also present in the CV curve during the first several hours after the gold electrode was immersed in the solution of **4**, *i.e.* the adsorption of the disulfide ligand on Au is a relatively slow process. During the reverse potential scan, a reoxidation peak of the thiolate anion at E_{pa} = –0.03 V was observed after the reduction peak of the Au^I—S bond (Fig. 3, *c*):

$$Au^I—S—R + e = Au^0 + {}^-S—R \ (E_{pc} = -0.82 \text{ V}),$$

$$R—S^- - e = R—S \ (E_{pa} = -0.03 \text{ V}).$$

The correctness of the peak assignments was supported by quantum chemical calculation of the change in the Gibbs energy of the cathodic and anodic reactions (ΔG). The calculated values of ΔG confirmed the interpretation of the voltammogram and were equal to –0.827 and –0.024 eV for the first and the second reactions, respectively.

No adsorption *via* the coordination of the Au atom by the nitrogen atoms of the terpyridine fragment at the initial moment of the contact of the electrode with the solution of **4** took place (peaks at E_{pc} from –1.4 to –1.5 V are absent in the CV curves). However, after ~20 h a peak at E_{pc} = –1.49 V corresponding to the reduction of the N-adsorbed ligand appeared in the CV curve.

Apparently, cobalt complex **18** based on ligand **4** has a polymeric structure in the crystalline state, and it is destroyed upon dissolution. According to the CV data, the structure of adsorbed complex **18** considerably differs from the structure of adsorbed complexes **12** and **13** but is similar to the structure of the complex formed upon keeping of the Au electrode with ligand **2** chemosorbed on it in the solution of $Co(ClO_4)_2$. The results obtained by CV show that the complex with a similar structure was formed on the surface by means of the reaction of ligand **4** adsorbed on the Au electrode with the solution of $Co(ClO_4)_2$. It can be suggested[20] that upon adsorption of complex **18**, a Co^{II} terpyridine complex with the ratio metal : ligand = = 1 : 1 is formed (Scheme 12). With time, some changes take place in the CV curve of the adsorbed complex **18**: after ~24 h, a strong enough peak at E_{pc} = –1.37 V corresponding to the reduction of N-adsorbed ligand appears in it. Apparently, the free ligand molecules, which are remained in the solution after the dissolution of polymeric complex **18** and their adsorption on the gold surface, undergo adsorption on the same surface in the competing process *via* binding to it by the terpyridine nitrogen atoms.

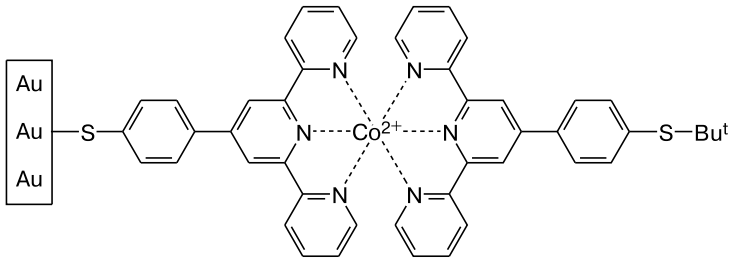

Fig. 6. Structure of complex **13** adsorbed on the gold surface.

Scheme 12

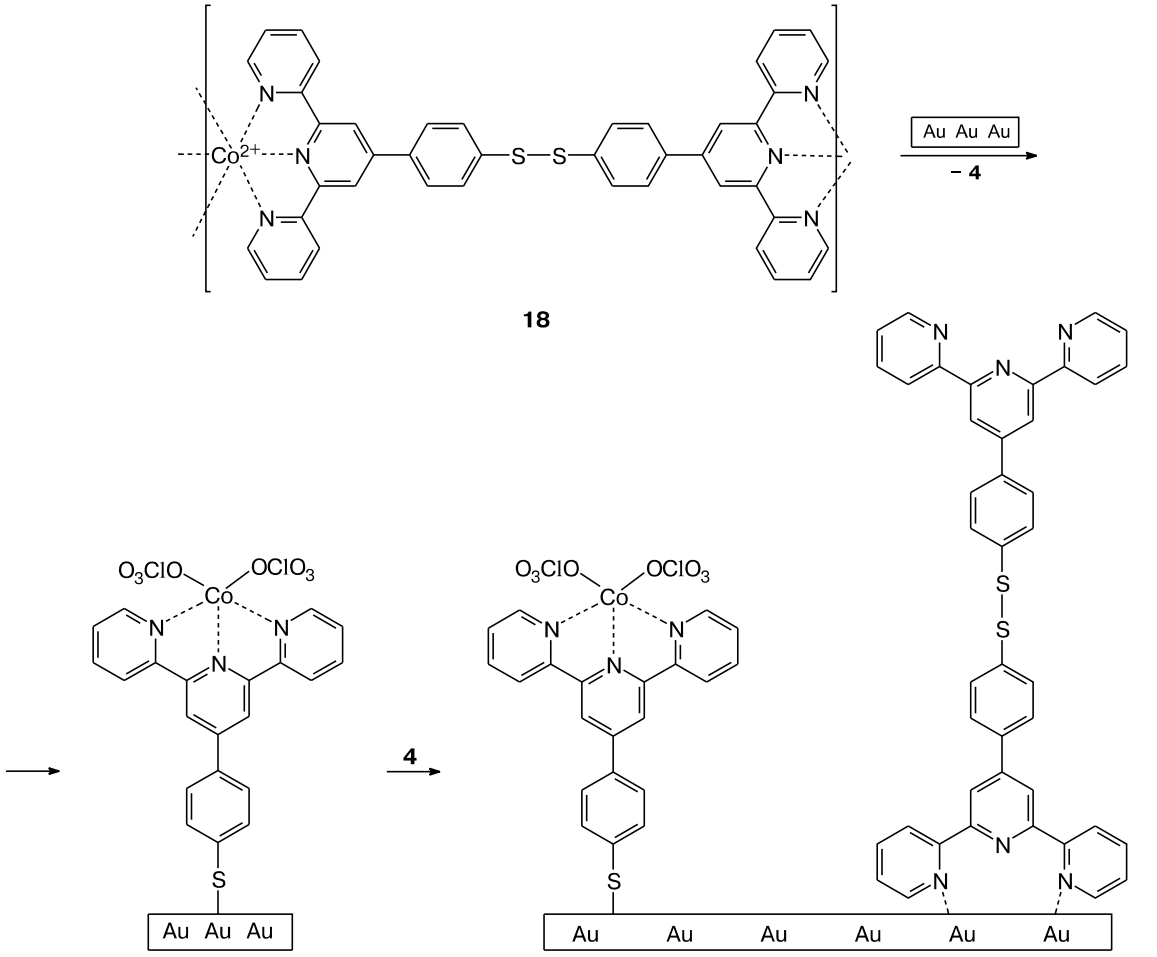

To sum up, a conclusion can be drawn that all the ligands studied are able to be chemosorbed on the surface of the gold electrode with the formation of the Au^{I}—S bond. The adsorption of the complexes of the sulfide ligands with Co^{II} follows different mechanisms. Thus, in the case of methylthio-substituted ligand **1**, the structure of the complex adsorbed on the surface is similar to its structure in solution, whereas in the case of *tert*-butylthio-substituted ligand **2**, the coordination polyhedron changes and the complex with the metal : terpyridines ligand ratio of 1 : 1 is formed upon adsorption.

Adsorption of coordination compounds of terpyridine ligands on the surface of gold nanoparticles. For the formation of NP dimeric and trimeric ensembles, we used a method suggested in our earlier study for the induction of aggregations through the coordination reactions of the ligands adsorbed on the surface of metallic nanoparticles with transition metal ions.[5] The structure of this dimeric aggregate is shown in Fig. 7.

There are two possible methods for the preparation of NP ensembles with such structures: one involves the interaction of NP modified by an organic ligand with solutions of transition metal salts; the second involves the adsorption on NP of preliminary obtained complexes of organic ligands with the same metal ions.

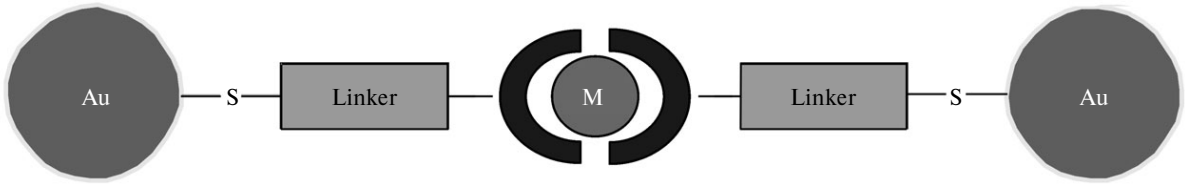

Fig. 7. Structure of gold NP dimeric aggregate.

We used the latter approach since, according to the electrochemical data and quantum chemical calculations, the synthesized terpyridine ligands can be adsorbed on the metal surface not only due to the formation of the S—Au bond, but also by means of the formation of the N—Au bond, that can lead to large aggregates by the interaction of the free ligands with gold NP. We studied the interaction of gold NP stabilized with citrate anions and tannic acid by the Turkevich method[21] with the Co^{II} coordination compounds (complexes **11**, **13**, **17**, **19**, and **24**), which resulted in obtaining of NP ensembles with different degrees of aggregation depending on the complexing ligand and the concentration of the solution of the complex. The structure and the size of the aggregates obtained were determined by electronic spectroscopy (from the position of the plasmon resonance band[22] in the electronic spectrum) and transmission electron microscopy.

Thus, the addition of a solution of complex **11** to a solution of stabilized gold NP led to a slight shift of the plasmon resonance band to the long-wavelength region in the electronic absorption spectrum (from 522 nm for the starting nanoparticles to 524 nm upon the addition of the complex), that indicated the formation of small aggregates. However, the electron microscopy data showed that in this case larger aggregates rather than dimers and trimers were mainly formed (Fig. 8). In addition, free unaggregated NP were observed in the micrographs.

For complex **13**, we studied the influence of the ratio of the terpyridine complex to gold nanoparticles on the aggregation process. The addition of a solution of complex **13** ($MeCN : H_2O = 1 : 9$, concentration 10^{-5} mol L^{-1}) to a solution of NP led to the immediate small shift of the plasmon resonance band to the long-wavelength region in the electronic absorption spectrum (from 516 to 519 nm), with its position and intensity remaining virtually unchanged henceforth (Fig. 9). The increase in the concentration of the complex to ~10^{-4}—10^{-3} mol L^{-1} led to a gradual broadening and shift of the plasmon resonance band toward the long-wavelength region by ~10—40 nm (see Fig. 9) indicative of the further agglomeration. The aggregates obtained in this case have proved unstable and after several hour after the formation, the polyaggregated NP precipitated from the solution.

According to the electronic spectroscopy data, under the optimal conditions (at the concentration of the solution of complex **13** ~10^{-5} mol L^{-1}), the dimerization process occurred within several minutes, and the aggregates formed in the solution remained stable for a long time (for at least 5 days). These conclusions were confirmed by the transmission electron microscopy data. Figure 10 shows the micrographs of the samples obtained for the gold NP in the course of aggregation caused by solutions of complex **13** of different concentrations.

Similar results were also observed in the studies of the interaction of gold NP with complex **19** containing a thiol group. In this case, stable small aggregates were obtained when the solution of the complex with the concentration of ~10^{-4} mol L^{-1} was used. In the electronic absorption spectrum of a solution of NP with this concentration of the aggregate-forming compound, a slight shift of the plasmon resonance bands toward the long-wavelength region was observed (from 520 to 525 nm). At the concentration of the complex ≥10^{-3} mol L^{-1}, the gold NP undergo aggregation to form small chain aggregates (Fig. 11).

Similar patterns were found in the study of the aggregation of gold NP under the action of compounds **17** and **24**. In this case, the maximum yield of dimeric aggregates

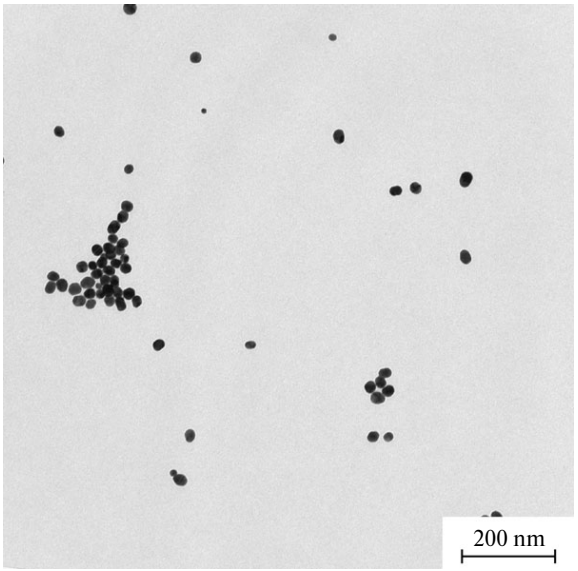

Fig. 8. Electron micrograph of gold NP modified with complex **11**.

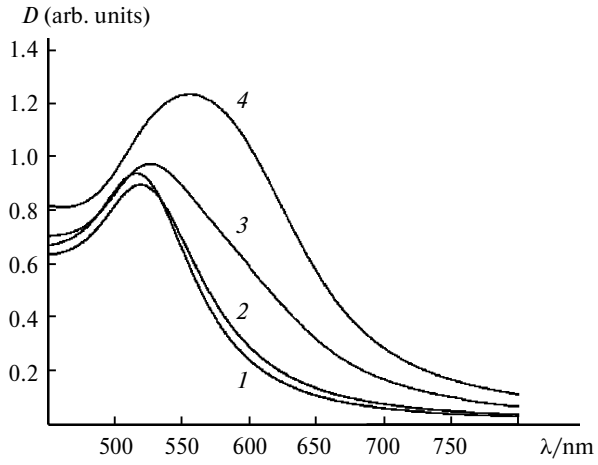

Fig. 9. Electronic absorption spectra of the starting gold NP (AuNP) (*1*) and gold NP treated with solutions of complex **13** (AuNP + **13**) with different concentrations: 10^{-5} (*2*), 10^{-4} (*3*), 10^{-3} mol L^{-1} (*4*).

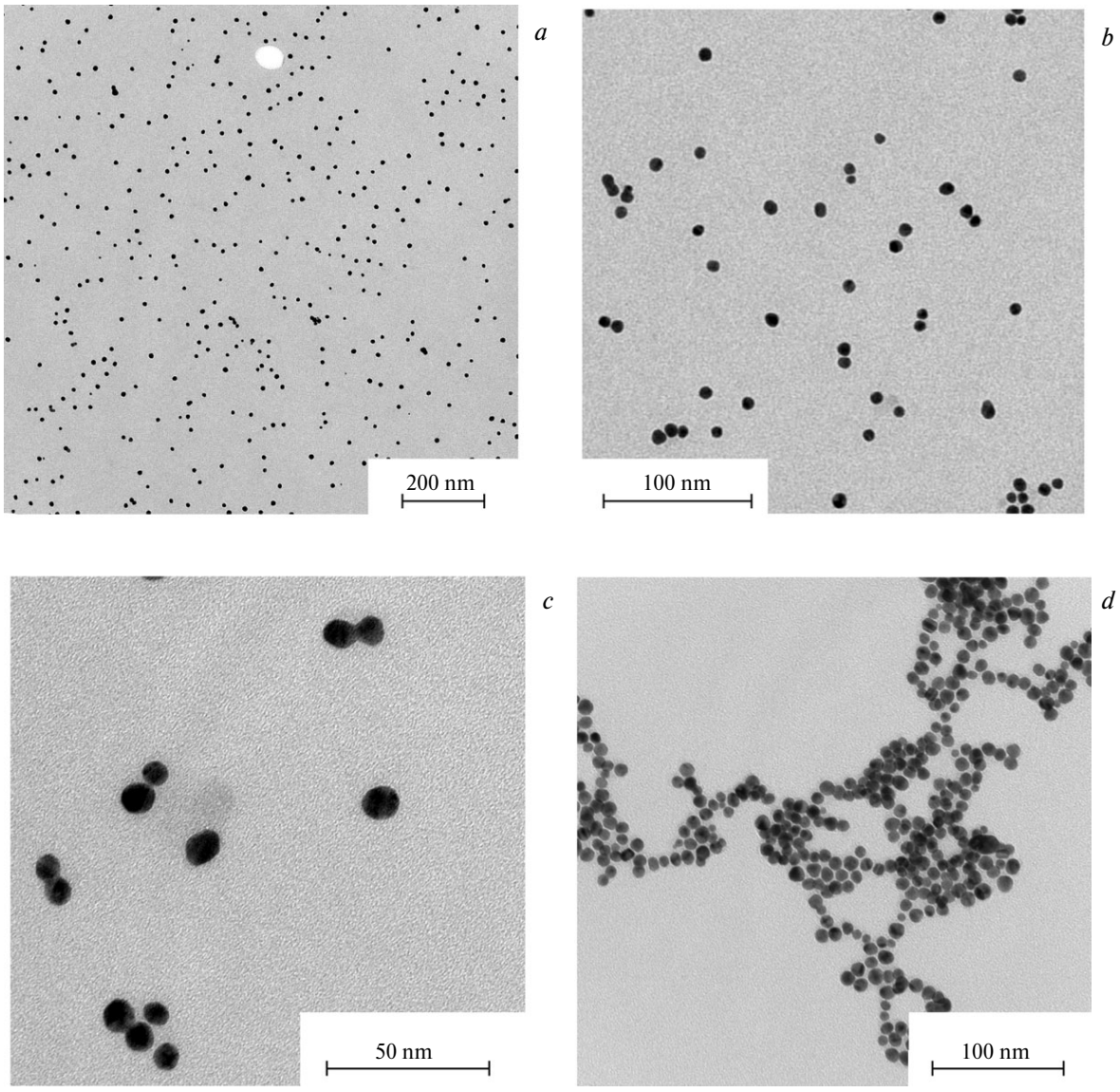

Fig. 10. Electron micrographs of gold NP samples: *a* the starting NP; *b*—*d* NP treated with solution of complex **13**: the concentration was ~10^{-5} (*b*, *c*) and ~10^{-4} mol L^{-1} (*d*).

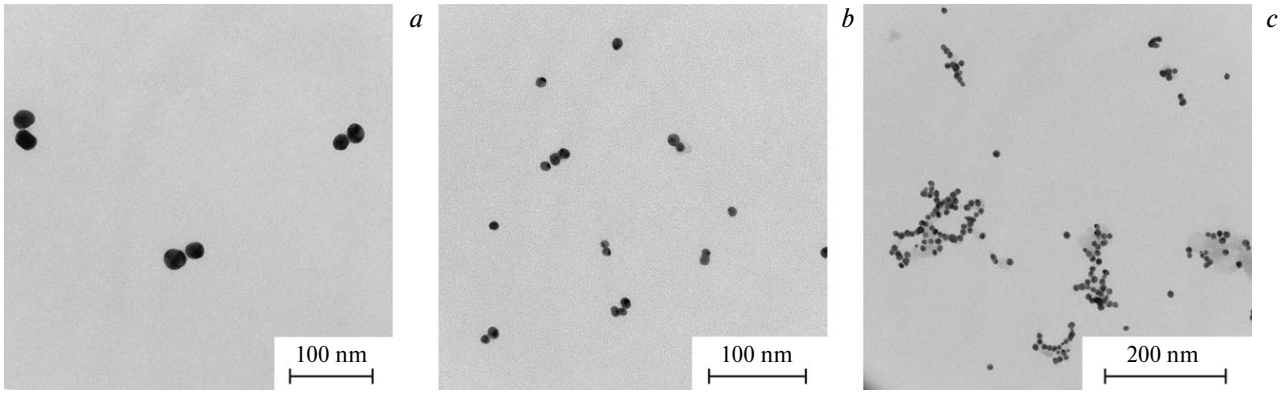

Fig. 11. Electron micrographs of gold NP samples treated with a solution of complex **19**: the concentration of the complex was ~10^{-4} (*a*, *b*) and ~10^{-3} mol L^{-1} (*c*).

was observed for solutions of complexes with the concentration of ~10^{-5} mol L^{-1}. In the electronic absorption spectra, the shift of the plasmon resonance band was 4—5 nm as compared to the starting NP obtained by the Turkevich method.

In conclusion, we developed conditions for the preparation of gold NP ensembles with different degrees of aggregation and found that the degree of NP aggregation was determined by the concentration of the terpyridine complex solution used for the preparation of the agglomerates. The use of a solution of the complex with the concentration of 10^{-4}—10^{-5} mol L^{-1} (depending on the type of the ligand) was found to be the optimal for the preparation of predominantly dimeric ensembles. The use of solutions of lower concentrations did not lead to the formation of aggregates, whereas excess of the complex initiated the formation of larger aggregates.

Experimental

The reaction progress and individuality of products were monitored by thin-layer chromatography on plates precoated with silica gel (Silufol).

^{1}H NMR spectra were recorded on a Bruker Avance spectrometer (400 MHz). Deuteriochloroform, dimethyl sulfoxide-d_6, and deuterobenzene-d_6 were used as solvents. Chemical shifts are given relative to hexamethyldisiloxane as an internal standard. ^{13}C and ^{31}P NMR spectra were recorded on a Bruker Avance spectrometer (100 MHz). IR spectra were measured on a UR-20 spectrometer in Nujol or on a TermoNicolete IR200 Fourier-transform infrared spectrometer in KBr pellets. The UV-Vis spectra were recorded on a Hitachi U-2900 spectrometer.

Laser ionization mass spectra were obtained on a Bruker Autoflex II (the FWHM resolution 18000) equipped with a nitrogen laser (operating at 337 nm wavelength) and a time-of-flight mass analyzer in the reflection mode. The accelerating voltage was 20 kV. Samples were deposited on a gold substrate. The spectra were recorded in the positive ion mode. The resulting spectrum was a sum of 300 spectra obtained at different sites of the sample.

X-ray diffraction study was performed on a CAD-4 automatic single-crystal diffractometer (graphite monochromator, λ(Mo-Kα) = 0.71073 Å, ω-scan technique). The structure was solved by direct methods (SHELXS-97)[23] and refined anisotropically by the full-matrix least squares method on F^2 for all the nonhydrogen atoms (SHELXL-97).[24] All the hydrogen atoms were located in Fourier maps and refined isotropically.

A PI-50-1.1 potentiostat connected to a PR-8 programmer was used for **electrochemical studies**. The working electrodes were glass-carbon (d = 2 mm), platinum (d = 2.8 mm), and gold (d = 2 mm) disks, the supporting electrolyte was 0.1 M Bu_4NBF_4 solution, the reference electrode was Ag/AgCl/KCl (sat.). The working electrode surfaces were polished with aluminum powder with a particle size less than 10 μ (Sigma-Aldrich). In the CV studies, the potential scan rate was 200 mV s^{-1}. All the measurements were carried out under argon. Samples were dissolved in the pre-deoxygenated solvent. Dimethylformamide (reagent grade) was stirred with anhydrous potassium carbonate (20 g L^{-1}) for 4 days at 20 °C, decanted, and further purified by consecutive reflux and distillation *in vacuo* over calcium hydride and anhydrous copper sulfate (10 g L^{-1}). The purified solvent was stored over 4 Å molecular sieves.

The sample **micrographs** were obtained on a LEO 912 AB OMEGA transmission electron microscope (Carl Zeiss, Germany) operating at an accelerating voltage of 100 kV. Samples were prepared by the deposition of 1—2 μL of the solution on a copper grid coated with Formvar (d = 3.05 mm), which was then dried in air.

4′-(4-Diethoxyphosphorylmethylphenyl)-2,2′:6′,2″-terpyridine (8) was obtained according to the known procedure.[25]

Quantum chemical calculations were performed using the Priroda 10 program[26] by the density functional theory (DFT) with the PBE (Perdew, Burke, Ernzerhow) nonempirical functional[27] using the all-electron λ-basis set.[28] Considerable gold relativistic effects were allowed for in terms of the relativistic approach with a modified Dirac—Coulomb—Breit Hamiltonian in the two-component approximation with renormalization of the large component of the bispinor.[29] Relative molecular energies were calculated with allowance for the zero-point vibrational energy in the harmonic approximation. The bond energies (E_b) of the substrate molecule R with the Au_n gold cluster were determined using the following formula:

$$E_b = E^0(Au_n) + E^0(R) - E^0(Au_nR),$$

where $E^0(Au_n)$, $E^0(R)$, and $E^0(Au_nR)$ are the total energies with allowance for the zero-point vibrational energy of the gold cluster, the molecule, and the molecule and cluster complex, respectively.

The changes in the Gibbs energy in the corresponding process were calculated at 298 K. The temperature correction for the Gibbs energy was determined by methods of statistical thermodynamics. The calculations were performed on the SKIF MSU Chebyshev supercomputer. Visualization of molecular orbitals was performed using the Molden software.

Synthesis of 4′-(4-methylsulfanylphenyl)-2,2′:6′,2″-terpyridine (1) and 4′-(4-*tert*-butylsulfanylphenyl)-2,2′:6′,2″-terpyridine (2) (general procedure). Potassium hydroxide and 25% aqueous ammonia were added to a solution of aldehyde and 2-acetylpyridine in EtOH. The solution obtained was stirred at room temperature for 12 h. The precipitate that formed was filtered off, washed with methanol, twice recrystallized from a methanol—dichloromethane mixture (1 : 1), and washed with cold diethyl ether.

4′-(4-Methylsulfanylphenyl)-2,2′:6′,2″-terpyridine (1). The reaction of 4-methylthiobenzaldehyde (2 g, 13.2 mmol), 2-acetylpyridine (3.2 g, 2.96 mL, 26.4 mmol), KOH (1.48 g, 26.4 mmol), and 25% aq. NH_3 (4.49 g, 4.99 mL, 66 mmol) in EtOH (40 mL) gave compound **1** (1.95 g, 42%). M.p. 176 °C. ^{1}H NMR (400 MHz, $CDCl_3$), δ: 8.75 (ddd, 2 H, $HC(6)_{Py}$, $HC(6'')_{Py}$, J_1 = 1.0 Hz, J_2 = 1.8 Hz, J_3 = 4.8 Hz); 8.74 (s, 2 H, HC(3′), $HC(5')_{Py}$); 8.68 (dt, 2 H, $HC(3)_{Py}$, $HC(3'')_{Py}$, J_1 = 1.0 Hz, J_2 = 7.9 Hz); 7.89 (dt, 2 H, $HC(4)_{Py}$, $HC(4'')_{Py}$, J_1 = 1.8 Hz, J_2 = 7.9 Hz); 7.87 (d, 2 H, $HC(2)_{C_6H_4}$, $HC(6)_{C_6H_4}$, J = 8.5 Hz); 7.39 (d, 2 H, $HC(3)_{C_6H_4}$, $HC(5)_{C_6H_4}$, J = 8.4 Hz); 7.37 (ddd, 2 H, $HC(5)_{Py}$, $HC(5'')_{Py}$, J_1 = 1.2 Hz, J_2 = 4.8 Hz, J_3 =7.6 Hz); 2.56 (s, 3 H, CH_3—S). Found (%): C, 74.29; H, 4.89; N, 11.78; S, 8.92. $C_{22}H_{17}N_3S$. Calculated (%): C, 74.37; H, 4.79; N, 11.83; S, 9.01.

4′-(4-*tert*-Butylsulfanylphenyl)-2,2′:6′,2″-terpyridine (2). The reaction of 4-(*tert*-butylthio)benzaldehyde (0.3 g, 1.5 mmol), 2-acetylpyridine (0.363 g, 0.336 mL, 3.0 mmol), KOH (0.168, 3.0 mmol), and 25% aq. NH_3 (0.567 mL) in EtOH (6 mL) gave compound **2** (0.27 g, 45%), m.p. 168 °C. ^{1}H NMR (400 MHz, $CDCl_3$), δ: 8.76 (s, 2 H, $HC(3')_{Py}$, $HC(5')_{Py}$); 8.74 (br.s, 2 H, $HC(6)_{Py}$, $HC(6'')_{Py}$); 8.70 (d, 2 H, $HC(3)_{Py}$, $HC(3'')_{Py}$, J = 8.0 Hz); 7.90 (dt, 2 H, $HC(4)_{Py}$, $HC(4'')_{Py}$, J_1 = 1.6 Hz, J_2 = 7.8 Hz); 7.88 (d, 2 H, $HC(2)_{C_6H_4}$, $HC(6)_{C_6H_4}$, J = 8.0 Hz); 7.69 (d, 2 H, $HC(3)_{C_6H_4}$, $HC(5)_{C_6H_4}$, J = 8.2 Hz); 7.38 (ddd, 2 H, $HC(5)_{Py}$, $HC(5'')_{Py}$, J_1 = 1.0 Hz, J_2 = 4.8 Hz, J_3 = 7.3 Hz); 1.35 (s, 9 H, $(CH_3)_3S$). Found (%): C, 75.44; H, 5.85; N, 10.41; S, 7.96. $C_{25}H_{23}N_3S$. Calculated (%): C, 75.57; H, 5.79; N, 10.58; S, 8.06.

4′-(4-Mercaptophenyl)-2,2′:6′,2″-terpyridine (3) and bis[1-(4-(2,2′:6′,2″-terpyridin-4′-yl)phenyl)]disulfide (4). A solution of compound **2** (0.33 g, 0.8 mmol) in 35% aq. HCl (56 mL) was stirred for 12 h at 90 °C under argon. The resulting solution was cooled to 0 °C, neutralized with 6 *M* NaOH to pH 8, and extracted with ethyl acetate. The solvent was evaporated under reduced pressure. According to the NMR spectroscopic data, the solid residue was a mixture of 4′-(4-mercaptophenyl)-2,2′:6′,2″-terpyridine (**3**) and bis{1-[4-(2,2′:6′,2″-terpyridin-4′-yl)phenyl]} disulfide (**4**). On storage in air, the mixture converted to pure disulfide **4**.

4′-(4-Mercaptophenyl)-2,2′:6′,2″-terpyridine (3). A suspension of triphenylphosphine (0.043 g, 0.16 mmol) in methanol (3 mL) was added to a vigorously stirred mixture of compounds **4** (0.075 g, 0.11 mmol) and **3** (0.15 g, 0.44 mmol) dissolved in degassed DMF (7 mL) under argon. The reaction mixture was stirred for 30 min followed by the addition of water (2 mL) and stirring for another 30 min. The resulting solution was cooled to 0 °C and extracted with diethyl ether (3×10 mL). The organic fractions were washed with cold water (2×5 10 mL) and dried with anhydrous sodium sulfate. The solvent was evaporated under reduced pressure. The product was isolated by flash chromatography in the light petroleum—ethyl acetate system (2 : 1). The solvents were evaporated under reduced pressure. The yield of compound **3** was 0.2 g (69%). ^{1}H NMR (400 MHz, $CDCl_3$), δ: 8.75 (ddd, 2 H, $HC(6)_{Py}$, $HC(6'')_{Py}$, J_1 = 1.0 Hz, J_1 = 1.8 Hz, J_3 = 4.9 Hz); 8.71 (s, 2 H, $HC(3')_{Py}$, $HC(5')_{Py}$); 8.68 (dt, 2 H, $HC(3)_{Py}$, $HC(3'')_{Py}$, J_1 = 1.8 Hz, J_2 = 7.6 Hz); 7.89 (dt, 2 H, $HC(4)_{Py}$, $HC(4'')_{Py}$, J_1 = 2.0 Hz, J_2 = 8.4 Hz); 7.81 (dt, 2 H, $HC(2)_{C_6H_4}$, $HC(6)_{C_6H_4}$, J_1 = 2.0 Hz, J_2 = 8.6 Hz); 7.41 (dd, 2 H, $HC(3)_{C_6H_4}$, $HC(5)_{C_6H_4}$, J_1 = 2.0 Hz, J_2 = 8.6 Hz); 7.37 (ddd, 2 H, $HC(5)_{Py}$, $HC(5'')_{Py}$, J_1 = 1.2 Hz, J_2 = 4.7 Hz, J_3 = 7.4 Hz); 3.59 (s, 1 H, SH). ^{13}C NMR (100 MHz, $CDCl_3$), δ: 149.1, 136.9, 128.1, 128.0, 123.8, 121.4, 121.3, 128.7. MS (laser ionization), m/z (I(%)): 342 (100 %) [MH^+].

Bis{1-[4-(2,2′:6′,2″-terpyridin-4′-yl)phenyl]} disulfide (4). The yield was 0.075 g (26%). M.p. 262 °C. ^{1}H NMR (400 MHz, $CDCl_3$), δ: 8.75 (m, 2 H, $HC(6)_{Py}$, $HC(6'')_{Py}$); 8.73 (s, 2 H, $HC(3')_{Py}$, $HC(5')_{Py}$), 8.69 (d, 2 H, $HC(3)_{Py}$, $HC(3'')_{Py}$, J = 8.0 Hz); 7.92 (m, 2 H, $HC(4)_{Py}$, $HC(4'')_{Py}$); 7.90 (d, 2 H, $HC(3)_{C_6H_4}$, $HC(5)_{C_6H_4}$, J = 7.6 Hz); 7.69 (d, 2 H, $HC(2)_{C_6H_4}$, $HC(6)_{C_6H_4}$, J = 8.4 Hz); 7.36 (dd, 2 H, $HC(5)_{Py}$, $HC(5'')_{Py}$, J_1 = 5.5 Hz, J_2 = 7.9 Hz). MS (laser ionization), m/z (I(%)): 681 (100 %) [MH^+].

4′-(4-Methylphenyl)-2,2′:6′,2″-terpyridine (5) was obtained according to the procedure described for compounds **1** and **2**. The reaction of 4-methylbenzaldehyde (3.5 g, 29.0 mmol), 2-acetylpyridine (7.02 g, 6.50 mL, 58.0 mmol), KOH (3.25 g, 58.0 mmol), and 25% aq. NH_3 (10.96 mL, 9.86 g, 145 mmol) in ethanol (80 mL) gave compound **5** (4.59 g, 49%), m.p. 174 °C. ^{1}H NMR (400 MHz, $CDCl_3$), δ: 8.76 (s, 2 H, $HC(3')_{Py}$, $HC(5')_{Py}$); 8.75 (br.s, 2 H, $HC(6)_{Py}$, $HC(6'')_{Py}$); 8.69 (d, 2 H, $HC(3)_{Py}$, $HC(3'')_{Py}$, J = 8.0 Hz); 7.89 (dt, 2 H, $HC(4)_{Py}$, $HC(4'')_{Py}$, J_1 = 1.6 Hz, J_2 = 7.7 Hz); 7.85 (d, 2 H, $HC(2)_{C_6H_4}$, $HC(6)_{C_6H_4}$, J = 8.1 Hz); 7.37 (ddd, 2 H, $HC(5)_{Py}$, $HC(5'')_{Py}$, J_1 = 1.0 Hz, J_2 = 4.9 Hz, J_3 = 6.5 Hz); 7.34 (d, 2 H, $HC(3)_{C_6H_4}$, $HC(5)_{C_6H_4}$, J = 8.0 Hz), 2.45 (s, 3 H, CH_3). Found (%): C, 81.68; H, 5.36; N, 12.94. $C_{22}H_{17}N_3$. Calculated (%): C, 81.73; H, 5.30; N, 13.00.

Reaction of 4′-(4-methylphenyl)-2,2′:6′,2″-terpyridine (5) with *N*-bromosuccinimide.[30] A suspension of compound **5** (2.5 g, 7.7 mmol), *N*-bromosuccinimide (1.64 g, 9.2 mmol), and AIBN (0.097 g, 0.6 mmol) in CCl_4 (25 mL) was refluxed for 2 h with stirring. The hot solution was filtered and the solvent was evaporated under reduced pressure. The resulting solid residue was a mixture of compounds **6** and **7**. To obtain an individual bromide **6**, the mixture was twice recrystallized from an ethanol—acetone mixture (2 : 1).

4′-(4-Bromomethylphenyl)-2,2′:6′,2″-terpyridine (6). The yield was 1.72 g (56%). M.p. 159 °C. ^{1}H NMR (400 MHz, $CDCl_3$), δ: 8.75 (br.s, 4 H, $HC(3)_{Py}$, $HC(6'')_{Py}$, $HC(6')_{Py}$, $HC(5')_{Py}$); 8.69 (d, 2 H, $HC(3)_{Py}$, $HC(3'')_{Py}$, J = 8.0 Hz); 7.91 (t, 2 H, $HC(4)_{Py}$, $HC(4'')_{Py}$, J = 7.7 Hz); 7.89 (d, 2 H, $HC_{C_6H_4}$, J = 8.3 Hz); 7.56 (d, 2 H, $HC_{C_6H_4}$, J = 8.1 Hz); 7.38 (ddd, 2 H, $HC(5)_{Py}$, $HC(5'')_{Py}$, J_1 = 1.0 Hz, J_2 = 4.8 Hz, J_2 = 7.2 Hz); 4.59 (s, 2 H, CH_2—Br). Found (%): C, 65.55; H, 4.11; N, 10.32. $C_{22}H_{16}BrN_3$. Calculated (%): C, 65.67; H, 3.98; N, 10.45.

4′-(4-Dibromomethylphenyl)-2,2′:6′,2″-terpyridine (7). The yield was 0.3 g (8%). M.p. 170 °C. ^{1}H NMR (400 MHz, $CDCl_3$), δ: 8.76 (br.s, 4 H, $HC(6)_{Py}$, $HC(6'')_{Py}$, $HC(3')_{Py}$, $HC(5')_{Py}$); 8.69 (d, 2 H, $HC(3)_{Py}$, $HC(3'')_{Py}$, J = 8.0 Hz); 7.90 (m, 4 H, $HC(4)_{Py}$, $HC(4'')_{Py}$, $HC_{C_6H_4}$); 7.73 (d, 2 H, $HC_{C_6H_4}$, J = 8.1 Hz); 7.39 (ddd, 2 H, $HC(5)_{Py}$, $HC(5'')_{Py}$, J_1 = 1.1 Hz, J_2 = 4.8 Hz, J_2 = 7.7 Hz); 6.74 (s, 1 H, CH—Br_2).

{4-[(*E*)-(2,2′:6′,2″-Terpyridin-4′-yl)phenylvinyl]phenyl} methyl sulfide (9) and {4-[(*E*)-(2,2′:6′,2″-terpyridin-4′-yl)-phenylvinyl]phenyl} *tert*-butyl sulfide (10) (general procedure). An aldehyde was added to a suspension of 4′-(4-diethoxyphosphorylmethylphenyl)-2,2′:6′,2″-terpyridine **8** and Bu^tOK in anhydrous degassed toluene (50 mL). The reaction mixture was refluxed for 48 h under argon. The resulting solution was washed with brine (3×20 mL), and the organic fractions were dried with anhydrous sodium sulfate. The solvent was evaporated under reduced pressure. The residue was dissolved in the dichloromethane : methanol system (40 : 1) and passed through a column-filter with silica gel. The solvent was evaporated under reduced pressure. The solution obtained was diluted with light petroleum—diethyl ether mixture (1 : 1) (5 mL), the precipitate that formed was filtered off.

{4-[(*E*)-(2,2′:6′,2″-Terpyridin-4′-yl)phenylvinyl]phenyl} methyl sulfide (9). The reaction of compound **8** (0.3 g, 0.6 mmol), Bu^tOK (0.073 g, 0.6 mmol), and 4-methylthiobenzaldehyde (0.099 g, 0.086 mL, 0.6 mmol) gave compound **9** (0.19 g, 64%), m.p. 262 °C. ^{1}H NMR (400 MHz, DMSO-d_6), δ: 8.77 (dd, 2 H, $HC(6)_{Py}$, $HC(6'')_{Py}$, J_1 = 1.6 Hz, J_2 = 4.7 Hz); 8.73 (s, 2 H, $HC(3')_{Py}$, $HC(5')_{Py}$); 8.66 (d, 2 H, $HC(3)_{Py}$, $HC(3'')_{Py}$, J = 8.0 Hz); 8.03 (dt, 2 H, $HC(4)_{Py}$, $HC(4'')_{Py}$, J_1 = 1.6 Hz, J_2 = 7.7 Hz), 7.94 (d, 2 H, $HC_{C_6H_4}$, J = 8.2 Hz); 7.80 (d, 2 H, $HC_{C_6H_4}$, J = 8.4 Hz); 7.60 (d, 2 H, $HC_{C_6H_4}$, J = 8.4 Hz); 7.52 (dd, 2 H, $HC(5)_{Py}$, $HC(5'')_{Py}$, J_1 = 4.9 Hz, J_2 = 6.6 Hz); 7.34 (d, 1 H,

HC=C, J = 15.6 Hz); 7.31 (d, 1 H, HC=C, J = 15.6 Hz); 7.28 (d, 2 H, $HC_{C_6H_4}$, J = 8.2 Hz); 2.47 (s, 3 H, CH_3—S). ^{13}C NMR (100 MHz, $CDCl_3$), δ: 156.3, 155.9, 149.1, 138.2, 136.9, 134.1, 128.9, 127.6, 127.0, 126.7, 123.9, 121.4, 118.5, 15.78. MS (ESI), m/z (I (%)): 458 (100) [MH^+]. Found (%): C, 78.82; H, 5.06; N, 9.08. $C_{30}H_{23}N_3S$. Calculated (%): C, 78.78; H, 5.03; N, 9.19.

{4-[(*E*)-(2,2′:6′,2″-Terpyridin-4′-yl)phenylvinyl]phenyl} *tert*-butyl sulfide (10). The reaction of compound **6** (0.3 g, 0.6 mmol), Bu^tOK (0.073 g, 0.6 mmol), and 4-(*tert*-butylthio)-benzaldehyde (0.126 g, 0.6 mmol) gave compound **10** (0.18 g, 57%). M.p. 182 °C. ^{1}H NMR (400 MHz, C_6D_6), δ: 9.33 (s, 2 H, $HC(3')_{Py}$, $HC(5')_{Py}$); 8.89 (d, 2 H, $HC(3)_{Py}$, $HC(3'')_{Py}$, J = 7.9 Hz); 8.72 (ddd, 2 H, $HC(6)_{Py}$, $HC(6'')_{Py}$, J_1 = 1.0 Hz, J_2 = 1.7 Hz, J_3 = 4.7 Hz); 7.77 (d, 2 H, $HC_{C_6H_4}$, J = 8.3 Hz); 7.67 (d, 2 H, $HC_{C_6H_4}$, J = 8.2 Hz); 7.45 (dt, 2 H, $HC(4)_{Py}$, $HC(4'')_{Py}$, J_1 = 1.8 Hz, J_2 = 7.8 Hz); 7.37 (d, 2 H, $HC_{C_6H_4}$, J = 8.4 Hz); 7.28 (d, 2 H, $HC_{C_6H_4}$, J = 8.3 Hz); 7.02 (d, 1 H, HC=C, J = 15.0 Hz); 6.99 (d, 1 H, HC=C, J = 15.1 Hz); 6.88 (ddd, 2 H, $HC(5)_{Py}$, $HC(5'')_{Py}$, J_1 = 1.0 Hz, J_2 = 4.7 Hz, J_3 = 7.4 Hz); 1.35 (s, 9 H, $(CH_3)_3S$). ^{13}C NMR (100 MHz, $CDCl_3$), δ: 156.2, 155.9, 149.1, 137.8, 136.9, 132.2, 128.9, 127.6, 127.1, 126.6, 123.8, 121.4, 118.5, 46.3, 31.0. MS (ESI), m/z I (%): 500 (100) [MH^+]. Found (%): C, 79.33; H, 5.83; N, 8.44. $C_{33}H_{29}N_3S$. Calculated (%): C, 79.36; H, 5.81; N, 8.42.

Bis[4′-(4-methylsulfanylphenyl)-2,2′:6′,2″-terpyridine]-cobalt(II) dihexafluorophosphate (11). A solution of ligand **1** (0.05 g, 0.14 mmol) and $Co(NO_3)_2 \cdot 6H_2O$ (0.02 g, 0.07 mmol) in methanol (40 mL) was refluxed with stirring for 12 h. The resulting solution was cooled and treated with a saturated solution of ammonium hexafluorophosphate in methanol. A dark red precipitate was filtered off and dissolved in minimum acetonitrile. Complex **11** was crystallized from the solution by a slow diffusion of diethyl ether into the solution of the complex in acetonitrile, m.p. >400 °C. Found (%): C, 49.75; H, 3.18; N, 7.88. $C_{44}H_{34}F_{12}N_6P_2S_2Co$. Calculated (%): C, 49.86; H, 3.21; N, 7.93.

Complexes with $Co(ClO_4)_2$ and $Ni(BF_4)_2$ (general procedure). A solution of the ligand and metal salt in methanol was refluxed with stirring for 12 h. The precipitate that formed was filtered off, washed with methanol and diethyl ether, and dried under reduced pressure.

Bis[4′-(4-methylsulfanylphenyl)-2,2′:6′,2″-terpyridine]-cobalt(II) diperchlorate (12). The reaction of ligand **1** (0.05 g, 0.14 mmol) and $Co(ClO_4)_2 \cdot 6H_2O$ (0.026 g, 0.07 mmol) in methanol (40 mL) gave complex **12** (0.060 g, 89%) as a finely crystalline claret-colored powder. M.p. >400 °C. Calculated (%): C, 54.54; H, 3.51; N, 8.68. $C_{44}H_{34}Cl_2N_6O_8S_2Co$. Found (%): C, 54.42; H, 3.67; N, 8.60.

Bis[4′-(4-*tert*-butylsulfanylphenyl)-2,2′:6′,2″-terpyridine]-cobalt(II) diperchlorate (13). The reaction of ligand **2** (0.05 g, 0.13 mmol) and $Co(ClO_4)_2 \cdot 6H_2O$ (0.023 g, 0.06 mmol) in methanol (40 mL) gave complex **13** (0.052 g, 83%) as a finely crystalline claret-colored powder, m.p. >400 °C. Calculated (%): C, 57.03; H, 4.37; N, 7.98. $C_{50}H_{46}Cl_2N_6O_8S_2Co$. Found (%): C, 56.97; H, 4.50; N, 8.01.

Bis[4′-(4-methylsulfanylphenyl)-2,2′:6′,2″-terpyridine]-nickel(II) ditetrafluoroborate (14). The reaction of ligand **1** (0.05 g, 0.14 mmol) and $Ni(BF_4)_2 \cdot 6H_2O$ (0.024 g, 0.07 mmol) in methanol (40 mL) gave complex **14** (0.40 g, 61%) as brown crystals suitable for X-ray diffraction analysis. M.p. >400 °C. Calculated (%): C, 55.99; H, 3.60; N, 8.91. $C_{44}H_{34}B_2F_8N_6S_2Ni$. Found (%): C, 55.90; H, 3.67; N, 8.70.

Bis[4′-(4-*tert*-butylsulfanylphenyl)-2,2′:6′,2″-terpyridine]-nickel(II) ditetrafluoroborate (15). The reaction of ligand **2** (0.025 g, 0.06 mmol) and $Ni(BF_4)_2 \cdot 6H_2O$ (0.011 g, 0.03 mmol) in methanol (15 mL) gave complex **15** (0.017 g, 57%) as a beige powder, m.p. >400 °C. Calculated (%): C, 58.42; H, 4.48; N, 8.18. $C_{50}H_{46}B_2F_8N_6S_2Ni$. Found (%): C, 58.61; H, 4.59; N, 8.13.

Bis({4-[(*E*)-(2,2′:6′,2″-terpyridin-4′-yl)phenylvinyl]phenyl} methyl sulfide)cobalt(II) diperchlorate (16). The reaction of ligand **9** (0.025 g, 0.06 mmol) and $Co(ClO_4)_2 \cdot 6H_2O$ (0.01 g, 0.03 mmol) in methanol (20 mL) gave complex **16** (0.026 g, 83%) as a claret-colored powder, m.p. >400 °C. Calculated (%): C, 61.43; H, 3.92; N, 7.17; S, 5.46. $C_{60}H_{46}Cl_2N_6O_8S_2Co$. Found (%): C, 61.23; H, 3.90; N, 7.18; S, 5.20.

Bis({4-[(*E*)-(2,2′:6′,2″-terpyridin-4′-yl)phenylvinyl]phenyl} *tert*-butyl sulfide)cobalt(II) diperchlorate (17). The reaction of ligand **10** (0.025 g, 0.05 mmol) and $Co(ClO_4)_2 \cdot 6H_2O$ (0.009 g, 0.025 mmol) in methanol (20 mL) gave complex **17** (0.025 g, 80%) as a claret-colored powder. M.p. >400 °C. Calculated (%): C, 63.06; H, 4.62; N, 6.69. $C_{66}H_{58}Cl_2N_6O_8S_2Co$. Found (%): C, 62.80; H, 4.76; N, 6.68.

({1-[4-(2,2′:6′,2″-Terpyridin-4′-yl)phenyl]} disulfide)cobalt(II) diperchlorate (18). The reaction of ligand **4** (0.020 g, 0.03 mmol) and $Co(ClO_4)_2 \cdot 6H_2O$ (0.011 g, 0.03 mmol) in methanol (10 mL) gave complex **18** (0.023 g, 82%) as a claret-colored powder. M.p. >400 °C. Calculated (%): C, 53.73; H, 2.98; N, 8.95. $C_{42}H_{28}Cl_2N_6O_8S_2Co$. Found (%): C, 53.56; H, 3.20; N, 8.94.

Bis[4′-(4-mercaptophenyl)-2,2′:6′,2″-terpyridine]cobalt(II) diperchlorate (19). The reaction of ligand **3** (0.025 g, 0.07 mmol) and $Co(ClO_4)_2 \cdot 6H_2O$ (0.013 g, 0.04 mmol) in methanol (15 mL) gave complex **19** (0.020 g, 58%) as a claret-colored powder, m.p. >400 °C. Calculated (%): C, 53.62; H, 3.19; N, 8.94; S, 6.81. $C_{42}H_{30}Cl_2N_6O_8S_2Co$. Found (%): C, 53.43; H, 3.32; N, 8.71; S, 6.55.

Preparation of compounds 21 and 22 (general procedure). A suspension of a ligand and $RhCl_3$ in ethanol—water mixture (2 : 1) was refluxed for 48 h. The precipitate that formed was filtered off, washed with methanol and diethyl ether, and dried in air.

{4′-[4-(Methylsulfanyl)phenyl]-2,2′:6′,2″-terpyridine}rhodium(III) trichloride (21). The reaction of ligand **1** (0.30 g, 0.84 mmol) and $RhCl_3$ (0.18 g, 0.84 mmol) gave complex **21** (0.17 g, 36%) as a dark green powder. M.p. >400 °C. Calculated (%): C, 46.77; H, 3.01; N, 7.44; S, 5.67. $C_{22}H_{17}Cl_3N_3SRh$. Found (%); C, 46.23; H, 3.53; N, 7.58; S, 5.12.

[4′-(4-*tert*-Butylsulfanylphenyl)-2,2′:6′,2″-terpyridine]-rhodium(III) trichloride (22). The reaction of ligand **2** (0.05 g, 0.13 mmol) and $RhCl_3$ (0.026 g, 0.13 mmol) gave complex **22** (0.024 g, 30%) as a dark brown powder, m.p. >400 °C. Calculated (%): C, 49.46; H, 3.79; N, 6.92; S, 5.28. $C_{25}H_{23}Cl_3N_3SRh$. Found (%); C, 48.99; H, 3.61; N, 6.50; S, 5.03.

Preparation of compounds 23 and 24 (general procedure). A suspension of complexes **21** or **22** and 1,4-bis(terpyridin-4′-yl)benzene (**20**) in an ethanol—water mixture (1 : 1) was refluxed with stirring for 18 h. The resulting mixture was filtered, a solution of ammonium hexafluorophosphate in water (1 mL) was added to the filtrate. The precipitate that formed was filtered off, washed with water, methanol, and diethyl ether, and dried under reduced pressure.

Bis{4′-[4-(methylsulfanyl)phenyl]-2,2′:6′,2″-terpyridine}[1,4-bis(terpyridin-4′-yl)benzene]dirhodium(III) hexakishexachlorophosphate (23). The reaction of complex **21** (0.05 g, 0.09 mmol) with 1,4-bis(terpyridin-4′-yl)benzene (0.024 g, 0.04 mmol) in an eth-

anol—water mixture (18 mL) and NH_4PF_6 (0.043 g, 0.27 mmol) gave complex **23** (0.046 g, 45%) as a yellow powder. M.p. >400 °C. EAS (10^{-6} *M* solution in CH_3CN), λ/nm (ε/L cm^{-1} mol^{-1}): 248 ($4.3 \cdot 10^4$); 290 ($9.8 \cdot 10^4$); 345 ($6.5 \cdot 10^4$); 362 ($7.0 \cdot 10^4$). Calculated (%): C, 41.27; H, 2.49; N, 7.22; S, 2.75. $C_{80}H_{58}F_{36}N_{12}P_6S_2Rh_2$. Found (%): C, 41.45; H, 2.87; N, 6.89; S, 3.24.

Bis{4′-[4-(*tert*-butylsulfanyl)phenyl]-2,2′:6′,2″-terpyridine}[1,4-bis(terpyridin-4′-yl)benzene]dirhodium(III) hexakishexachlorophosphate (24). The reaction of complex **22** (0.025 g, 0.04 mmol) with 1,4-bis(terpyridin-4′-yl)benzene (0.011 g, 0.02 mmol) in an ethanol—water mixture (9 mL) and NH_4PF_6 (0.02 g, 0.12 mmol) gave complex **24** (0.05 g, 44%) as a brown powder. M.p. >400 °C. EAS (10^{-6} *M* solution in CH_3CN), λ/nm (ε/L cm^{-1} mol^{-1}): 247 ($4.3 \cdot 10^4$); 291 ($9.7 \cdot 10^4$); 344 ($6.6 \cdot 10^4$); 361 ($7.0 \cdot 10^4$). Calculated (%): C, 42.82; H, 2.90; N, 6.97; S, 2.65. $C_{86}H_{70}F_{36}N_{12}P_6S_2Rh_2$. Found (%): C, 42.17; H, 2.99; N, 6.86; S, 2.02.

Synthesis of modified gold NP

Nanoparticles stabilized with sodium citrate and tannic acid (Turkevich method). A solution of compound **1**, 1% aq. $HAuCl_4 \cdot 3H_2O$ (1 mL), and distilled water (80 mL) was heated to 60 °C. The resulting hot solution was diluted with vigorous stirring with a solution of 1% aq. sodium citrate (4 mL), 1% aq. tannic acid (0.08 mL), and distilled water (15 mL) preliminary heated to 60 °C. The solution obtained was refluxed for 2 h (until the solution acquired red color). Then the solution was cooled to room temperature with stirring. The resulting solution of gold NP was stored at about 4 °C. Further the NP stabilized with sodium citrate and tannic acid were involved in the reaction with appropriate sulfur-containing ligands and complexes.

Nanoparticles modified with {4-[(*E*)-(2,2′:6′,2″-terpyridin-4′-yl)phenylvinyl]phenyl} *tert*-butyl sulfide (2). The reaction of $HAuCl_4 \cdot 3H_2O$ (0.2 g, 0.56 mmol) in distilled water (20 mL), tetraoctylammonium bromide (0.342 g, 0.63 mmol) in toluene (15 mL), **2** (0.056 g, 0.11 mmol) in toluene (2 mL), and sodium borohydride (0.234 g, 6.2 mmol) in distilled water (14 mL) gave modified gold NP (0.16 g).

Reaction of gold nanoparticles stabilized with sodium citrate and tannic acid with terpyridine cobalt(II) complexes (general procedure). A solution of a complex (**11**, **13**, **17**, **19**, and **24**) in acetonitrile (100 μL) (complexes **11**, **13**, **17**, and **24**) or dimethylformamide (complex **19**) at the concentration of 10^{-2}, 10^{-3}, or 10^{-4} mol L^{-1} was mixed with distilled water (900 μL). A solution of gold NP (1.25 mL) stabilized by Turkevich method was diluted twofold with distilled water. A solution of the complex (100 μL) was added to the obtained solution of gold NP (2.5 mL). The resulting samples were studied by UV-Vis and transmission electron microscopy.

This work was financially supported by the Russian Foundation for Basic Research (Project No. 10-03-00707a).

References

1. M.-C. Daniel, D. Astruc, *Chem. Rev.*, 2004, **104**, 293.
2. A. C. Templeton, W. P. Wuelfing, R. W. Murray, *Acc. Chem. Res.*, 2000, **33**, 27.
3. G. Schmid, M. Baumle, M. Greekens, I. Heim, C. Osemann, T. Sawitowski, *Chem. Soc. Rev.*, 1999, **28**, 179.
4. A. Ulman, *Chem. Rev.*, 1996, **96**, 1533.
5. R. B. Romashkina, E. K. Beloglazkina, A. N. Khlobystov, A. G. Majouga, D. A. Pichugina, V. I. Terenin, N. V. Zyk, N. S. Zefirov, *Mendeleev Commun.*, 2011, **21**, 129.
6. D. Zanchet, C. M. Micheel, W. J. Parak, D. Gerion, S. C. Williams, A. P. Alivisatos, *J. Phys. Chem. B.*, 2002, **106**, 11758.
7. T. H. Galow, A. K. Boal, V. M. Rotello, *Adv. Mater.*, 2000, **12**, 576.
8. H. Yao, H. Kojima, S. Sato, K. Kimura, *Langmuir*, 2004, **20**, 10317.
9. R. Sardar, T. B. Heap, J. S. Shumaker-Parry, *J. Am. Chem. Soc.*, 2007, **129**, 5356.
10. E. C. Constable, M. D. Ward, *J. Chem. Soc., Dalton Trans.*, 1990, 1405.
11. M. Ziegler, V. Moneey, H. Stoeckli-Evans, A. Von Zelewsky, I. Sasaki, G. Dupic, J.-C. Daran, G. G. A. Balavoine, *J. Chem. Soc., Dalton Trans.*, 1999, 667.
12. J. Paul, S. Spey, H. Adams, J. A. Thomas, *Inorg. Chim. Acta*, 2004, **357**, 2827.
13. M. Maestri, N. Armaroli, V. Balzani, E. C. Constable, A. M. W. Cargill Thompson, *Inorg. Chem.*, 1995, **34**, 2759.
14. M. Beley, J. P. Collin, R. Louis, B. Metz, J. P. Sauvage, *J. Am. Chem. Soc.*, 1991, **113**, 8521.
15. E. K. Beloglazkina, A. G. Majouga, R. D. Rakhimov, N. V. Zyk, *Russ. J. Gen. Chem.* (*Engl. Transl.*), 2010, **80** [*Zh. Obshch. Khim.*, 2010, **80**, 201].
16. E. K. Beloglazkina, A. G. Majouga, I. V. Yudin, R. D. Rahimov, B. N. Tarasevich, N. V. Zyk, *J. Sulfur. Chem.*, 2007, **28**, 201.
17. E. K. Beloglazkina, A. G. Majouga, A. A. Moiseeva, M. G. Tsepkov, N. V. Zyk, *Russ. Chem. Bull. (Int. Ed.)*, 2007, 351 [*Izv. Akad. Nauk, Ser. Khim.*, 2007, 339].
18. L. S. Pinheiro, M. L. A. Temperini, *Surface Science*, 2000, **464**, 176.
19. J. Li, X. Li, H.-J. Zhai, *Science*, 2003, **299**, 864.
20. M. Maskus, H. D. Abruna, *Langmuir*, 1996, **12**, 4455.
21. J. Turkevich, P. C. Stevenson, J. Hillier, *Discuss. Faraday Soc.*, 1951, **11**, 55.
22. S. P. Gubin, N. A. Kataeva, G. Yu. Yurkov, *Nanochastitsy blagorodnykh metallov i materialy na ikh osnove* [*Nanoparticles of Noble Metals and Materials on Their Basis*] N. S. Kurnakov Institute of General and Inorganic Chemistry of Russian Academy of Sciences, Moscow, 2006, 155 pp. (in Russian).
23. M. Sheldrick, *Acta. crystallogr. Sect. A*, 1990, **46**, 467.
24. G. M. Sheldrick, *SHELXL-97. Program for the Refinement of Crystal Structures, University of Gottingen*, Gottingen, Germany, 1997.
25. A. Winter, D. A. M. Egbe, U. S. Schubert, *Org. Lett.*, 2007, **9**, 2345.
26. D. N. Laikov, *PRIRODA, Electronic Structure Code, Version 10*, 2010.
27. J. P. Perdew, K. Burke, M. Ernzerhoff, *Phys. Rev. Lett.*, 1996, **77**, 3865.
28. D. N. Laikov, *Chem. Phys. Lett.*, 2005, **416**, 116.
29. K. G. Dyall, *J. Chem. Phys.*, 1994, **100**, 2118.
30. H. L. Smith, R. L. Usala, E. W. McQueen, J. I. Goldsmith, *Langmuir*, 2010, **26**, 3342.

Received June 28, 2011;
in revised form November 14, 2012